1 Introduction

1.1 The need for stray-field mitigation

The goal of the international Muon Ionisation Cooling Experiment[1] is to construct a section of cooling channel long enough to demonstrate a measurable cooling effect. This is achieved by reducing the transverse emittance of a muon beam by the order of 10%.

A range of particle detectors will be used to measure the cooling effect particle by particle with high precision, in order to achieve an absolute accuracy on the measurement of emittance of 0.1% or better. The emittance measurements will be performed with muon beams of various momenta within the range of 140 to 240 MeV/c and a variety of beam optics and absorber materials will be employed.

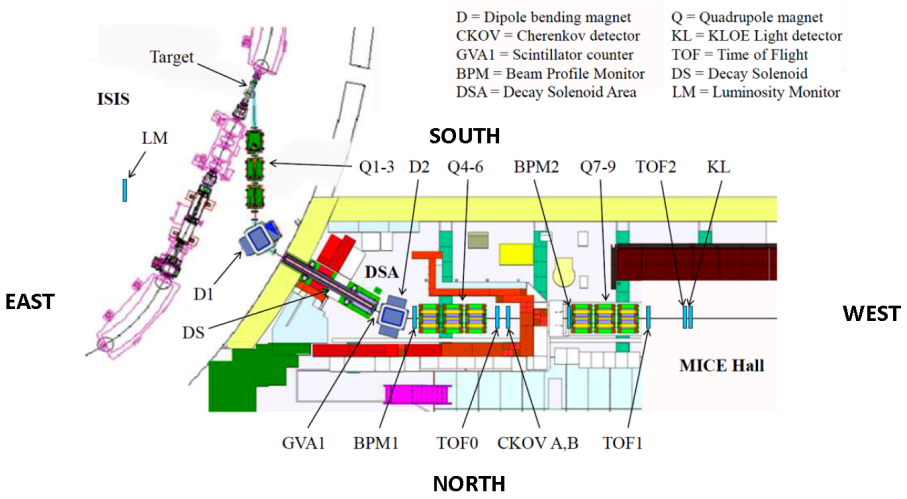

Figure 1: Schematic diagram of the MICE beamline.

To achieve this aim the MICE cooling channel is being built in several steps. Step I, the construction of the primary beamline has been completed, and commissioning studies of this beamline have been undertaken [DO WE NEED A REFERENCE HERE - AND WHICH ONE DO WE USE?]. Step II and III have been coalesced into Step IV. Step IV will see the introduction of the first of the cooling channel superconducting solenoids into the MICE hall with the installation of the spectrometer solenoids (SS1 and SS2) and

the first of three absorber focus coils (AFC). Step VI will see the addition of two more focus coils and two coupling coils.

Figure 1 shows a schematic layout of the MICE beamline. This figure also shows the relative directions of North, South, East and West with respect to the hall, these directions are referenced frequently throughout this document. Figure 2 illustrates the magnet layout of the cooling channel for Step's IV and VI and the timeline for these steps based upon the current schedule. Figure 3 is an impression of the full cooling channel at Step VI.

The MICE cooling channel magnets will produce significant fields, with each magnet typically producing a field of the order of several Tesla. The cooling channel will be run in one of two configurations, solenoid or flip mode. In solenoid mode, as the name suggests, the magnets will be powered in such a way to ensure that the field throughout the entire cooling channel is solenoidal. In flip mode the field throughout the cooling channel will be periodically reversed. This field reversal will take place at the second coil in each AFC magnet. The precision of the emittance measurement is determined by the trackers, however flipping thew field presents a different lattice configuration and so a test of how well the lattice is understood.

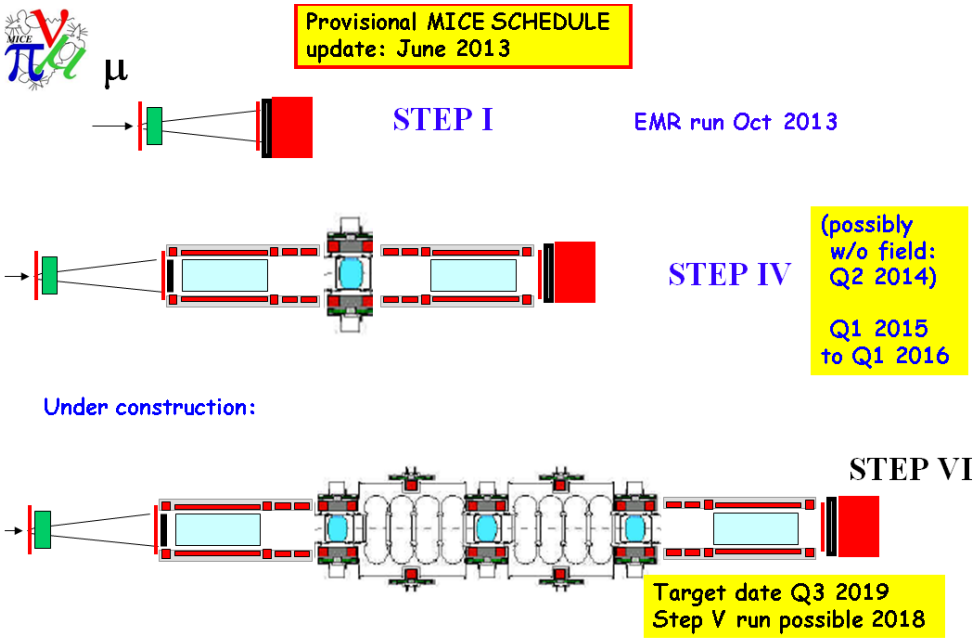

Figure 2: Schematic diagram of the MICE beamline.

It is worth noting at this point that the coupling coils are large bore magnets

and it is expected, and models indicate, that these will add significantly to the stray field produced by the MICE magnets.

In order to contain the stray field within the MICE hall two shield walls were built to contain the field within the confines of the MICE hall. These walls, the North and South Shield Walls have been constructed and are now a structural part of the MICE experiment. However there have been two problems.

1) The gradual creep of equipment into the volume contained by the shielded area.

2) The realisation that the extent of the stray field from the cooling channel magnets may be higher than original simulations had indicated. There is a concern that the shield walls may not be sufficiently large enough to contain the stray field. If this is the case then there may be a cause to be concerned about the effect of the stray field on equipment and people outside of the shielded zone.

It is important that neither of these issues prevents the experiment from operating and defining a scheme that both addresses and solves these issues is imperative to the success of the experiment.

For MICE itself, obtaining timely data at Step IV is critical to the success of the experiment, therefore finding a solution that permits Step IV to proceed in a punctual manner is clearly of upmost priority. A solution that naturally extends beyond Step IV and could be utilised for Step VI is also of merit. In practice we see the need to fulfill four requirements so that MICE can proceed to take data once the superconducting magnets are installed and operating:

1) We need to find a solution that permits the MICE magnets to be utilised to their full operating currents, in both flip and solenoid mode for Step IV of the experiment.

2) The solution must be practical, insomuch that it must not place unreasonable constraints upon the ability to operate the experiment both in terms of physical access to the various components of the experiment and the amount of time it takes to run the experiment.

3) All equipment belonging to MICE and ISIS must function normally. Not only does this include equipment that is specific to the experiment itself but also covers the infrastructure that supports the experiment and the surrounding buildings.

4) All health and safety requirements with respect to personnel safety in magnetic fields must be adhered to.

There is a significant amount of equipment required to run the MICE experiment and it is important that the stray field from the magnets does not interfere with its functioning. Not only does this include the equipment that directly runs the experiment but consideration must also be given to all the infrastructure equipment, such as fire safety, personnel safety, etc. Establishing what equipment could be affected and the field limits at which this equipment can operate is a necessary prerequisite to understanding the extent of the remedial work which needs to be undertaken. In the cases where there is a clear problem it will be necessary to either shield or move the equipment. How this is done will be discussed in this report.

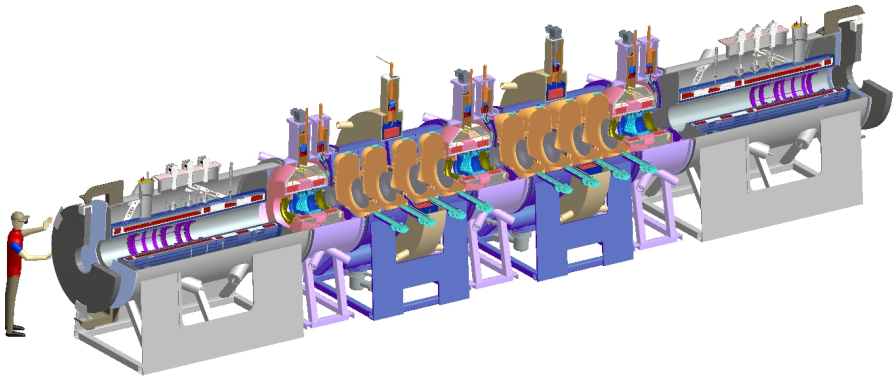

Figure 3: Schematic diagram of the MICE cooling channel.

It is also of material relevance that the ISIS control room is located next to the MICE control room. It will be necessary to demonstrate that the field levels within the ISIS control room are at a level that ensures that the control equipment in those rooms is not adversely affected. More generally MICE must demonstrate that it does not produce stray fields that interfere with any other equipment that is not within its remit.

The RAL & CERN 'Best Practice' guide impose a magnetic field limit of five gauss to areas that are accessible to the public [CRAIG CAN YOU FIND A REF FOR THIS?] due to the possibility that member of the public with pacemakers may be present. It is clear that any solution presented demonstrates that there are no fields above five gauss in areas that are accessible to the

public. In the case of the MICE experiment 'public' can be regarded as being in any non-controlled area of the experiment so this is effectively anywhere outside of the MICE Hall.

2 Magnetic Modelling of the MICE Hall

2.1 Purpose of the Model

In order to further understand the issues with the stray field of the MICE magnets it was deemed prudent to build a magnetic model of the MICE hall to give us further insight into the likely effect of the stray field throughout and beyond the volume of the MICE hall. This model should be capable of producing field maps for the various operating modes of the MICE magnets; and in the first instance with emphasis on Step IV of the experiment. More succinctly the aims were to:

1) Produce field maps that would permit a better understanding of potential issues arising within the hall from not having a return yoke on the cooling channel magnets. This in turn would guide the necessary mitigation work for the baseline design.

2) To use these field maps as input into other models.

3) To allow members of the collaboration to have access to estimates of the likely field levels in the vicinity of their equipment.

The following section details a description of the magnetic model of the MICE hall. How the model interfaces with the Baseline plan is discussed later.

2.2 Introduction

The MICE hall represents a significant volume of approximately 40 m $\times$ 12 m $\times$ 12 m and contains a significant amount of ferrous material. There is no symmetry to exploit. There is also much interest in how the fields penetrate beyond the confines of the MICE hall, particularly on the South Side, and given that a significant additional volume is required to ensure that the boundary does not influence the solution it is clear that the extent of the model is substantial. The total volume of the model has turned out to be approximately 120 m $\times$ 80 m $\times$ 80 m.

Building an FEA model on this scale requires a careful balance between detail and mesh size. This means that certain ferrous objects have not been modelled and in some cases some detail in the objects has been omitted to make the problem tractable. Nonetheless the model is still large and takes significant computing resources to solve.

The software package used to generate the magnetic FEA model is called OPERA, which is a commercially available software package. The geometry and model setup is defined in a module called the 'modeller'. This module also meshes the complete model after the geometry of the model has been built. For complex geometry the entire model, setup and meshing is invariably defined in a user defined file called .comi code, this is a scripting language that allows you to drive OPERA. After meshing the model is passed to the solver module which iteratively finds a solution to the problem. The solved problem can then analysed in a further module called the 'post-processor'.

Vector Fields were consulted to look at the model and give their opinion on the accuracy of the model, details of this will be discussed in the later section 2.7. However it is worth pointing out that the general consensus was that the model was well put together and that any errors due to modelling technicalities should be minimal. Of course this result is independent and separate to the issue of accurate geometric representation of ferrous components and whether we have an accurate representation of all ferrous mass in the model, the latter being quite difficult to judge and remains an uncertainty. More will be stated on this in section 2.4.

Finally, before looking at specifics, it is worth noting that there is a significant database of additional information on the web. All the models that have been built, code, drawings that have been used, personal notes, images generated from the model, and other details have been placed at the following website:

http://www.hep.shef.ac.uk/research/mice/opera_models/

2.3 Magnets

The magnets for the hall model were taken from a set of conductor files that had been used in previous models. These files define the geometry for the step IV and step VI magnets and the currents through them for flip and solenoid mode for 240 MeV/c operation. The hall model has only ever been run with 240 MeV/c settings as this gives the highest magnet currents and therefore the highest stray fields.

The magnet files define the magnet geometries and currents to be those as defined in the MICE technical reference document (TRD)[2]. These values may differ from the 'as-built' magnets slightly, as construction of the magnets has in certain cases lead to small discrepancies in the geometry and current densities. However as the final fields will in either case be identical, this should be of no real consequence to the modelling.

2.4 Objects in the Model

Both ferrous and non-ferrous items exist in the model. Technically there is no need to add the non-ferrous items, however on a model of this size and complexity, those items provide useful reference structures. Consequently the geometry of the non-ferrous items may be less critical, although their proximity to the MICE magnets is still important if they are being used as such. A more thorough description is given to the included ferrous items, although more detail can be found by consulting the technical drawings and the .comi code.

Throughout this document the various walls and components of the MICE hall are referenced via their geographic location, i.e. north, south, east and west. These directions were shown on figure 1. To help aid the reader to reference themselves figure 4 also shows the these directions with respect to an illustration of a MICE hall model 91.

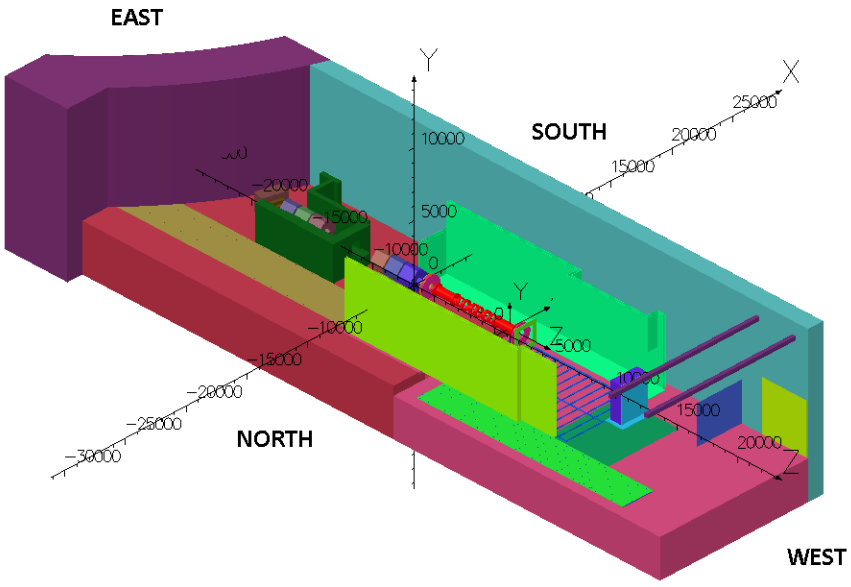

Figure 4: Relative orientation of the MICE Hall superimposed onto Model 91. Note that some structures from this model have been removed in this figure.

2.4.1 Ferrous Objects

Here are listed the main ferrous objects that have been included in the hall model and some relevant notes as to their description and function for refer-

ence.

North and South Shield Walls (NSW and SSW)

The North and South Shield Walls are modelled as a continuous double skinned wall, each skin composed of 35 mm AISI 1010 steel. The floor plates on the SSW are flat whereas in reality they are inclined. This means there is a small amount of missing steel in model of the SSW model, this is the steel that would fill in the gap where the floor actually slopes.

The I beams that support the shield wall are not modelled, this is a significant amount of steelwork but this level of detail could not be supported in the hall model.

Floor Web and Floor Web Plates

This is an estimate of the lattice steelwork that sits underneath the beamline between the NSW and SSW. There is also some lattice steel work on the North side of the NSW and the steel floorplates that sit on top of this.

Dipole D2

The dipole is modelled as a solid block of steel. The dipole functionality, i.e. its coils, have not been included in the model.

Quadrupoles, Bases and Baseplates

Q4-Q9 have been included in the model, including an estimation of the steelwork in their bases and the baseplates, which was considered significant. Like the dipole, the quad functionality, i.e. coils, has not been included in the model. As the quadrupoles have been modelled as a lumped mass of ferrous material there is a slight concern that their ferrous mass may have been overestimated.

Virostek Plates and Upstream TOF plates

The purpose of the Virostek plates is to sheild the photomultiplier tubes in the TOF detectors from the stray magnetic field. The upstream TOF plate

sandwiches the TOF1 detector between the TOF plate and the Virostek plate improving the the shielding for the TOF1 photomultipliers.

*** (Why is there no TOF plate for TOF 2? - I don't know) ***

The Electron Muon Ranger - EMR

A simple frame has been included to represent the EMR steelwork. The framework for the EMR is complex and would have been difficult to model in detail.

Decay Solenoid Area - DSA

The DSA is wall composed of steel and concrete blocks that seperates the decay solenoid, D2, Q4-Q6 from the rest of the MICE hall. The DSA comes under the province of ISIS and is considered to be part of the synchrotron space, access to this area is limited during ISIS operation. The steelwork that forms the DSA area constitutes a signficant mass of steel and therefore this has been included in the MICE hall model.

Beam Dump

The beamdump is a steel and concrete assembly that marks the end of the MICE beamline. The model was based upon the technical drawings, although some of the outer steel framing was missed off due to resolution limitations in the model.

South West Distribution Board

Although this only a small amount of steel this was included in the hall model as there is some electrical installation attached to the wall.

Linac Shield Wall

The linac wall is a steel loaded concrete wall and provides shielding from the ISIS linac room which runs parallel to the MICE experimental hall. This wall was modelled with a reduced BH curve to approximate its reduced gross magnetisation. The reduced BH curve was calculated from comparing the

attractive force of a magnet to the linac wall, and scaling this to the force measured for the shield wall (AISI 1010 steel). This is a crude technique but gives a reasonable first approximation to the magnetisation. In the hall model the linac wall has been assigned a reduced mild steel BH curve. The magnetisation of this curve has been reduced to 15% of its nominal value.

Trench Plates

The plates covering the Trench are currently steel; as they constitute a significant amount of steel and run in the z direction they were included in the model. There is also a considerable amount of structural steelwork beneath these plates that has not been included in the model.

Cellar

There was some concern over the effect of eight magnet bases that had been buried in the MICE hall. For this reason these bases were included in the model. These bases are steel shells that are concrete filled.

North Mezzanine

The north Mezzanine floor runs behind the north shield wall and is currently constructed from steel plate, so these plates were added to the model. The structural steelwork supporting this floor was not added to the model.

Cranes

The two cranes were crudely approximated by two steel beams that run North to South in the West end of the MICE hall. This should give a reasonable approximation to their ferrous mass, but their geometry, which is complex, is not approximated.

Return Yoke

An option was added to the model to run it with a return yoke that looks very similar to some of Holger Witte's early designs. The return yoke in the

hall model has 12 cm thick walls. The .comi code can be configured to both attach the yoke to the Virostek Plates and to include an extended flange.

2.4.2 Missing Ferrous

As pointed out previously in a model of this size some compromises have had to be made and consequently there is missing ferrous content in the model. There will be a significant number of small ferrous objects that would have been impractical to document and model. In terms of known missing ferrous that may be of significance this includes:

I Beams - Structural steels for Walls and Floors.
Any Cabinets/Compressors/Racks and Contents
Substation
Fridge Equipment

Unknown Ferrous - Iron objects below a critical size that have not been examined. Additional Iron in the DSA area? (Although this shouldn't be too relevant as the field in this area is not of concern.)

2.4.3 Non-Ferrous Structures

Due to the size of the model many non-ferrous structures were added as reference points in the model. These structures make it much easier to determine the field level in a particular volume of the MICE hall without having to refer to a coordinate system, which can be prone to error if entered manually. The main objects of note are:

Floors Walls and Roof of MICE Hall

Trench - This sits in the floor at the east end of the MICE Hall. As there is equipment in the trench it seemed prudent to add this space to the model.

South Side Buildings - This is the name given to the collection of rooms/buildings that are on the south-side of the MICE hall. These rooms are of particular interest as they will contain equipment that could be sensitive to stray field. The rooms include, The MICE local control room, hydrogen room, proposed Rack Room 2, the ISIS plant room and the three ISIS control rooms.

2.5 Code Structure and Meshing

The code structure for building the MICE hall model modular, each component in the MICE hall has its own set of .comi scripts. A master file controls which of the above components are built or not. Primarily this feature was added to aid debugging but in principle it also allows simpler models to be run. Geometry and mesh information are stored in separate files, which allows for this information to be easily edited.

2.6 Solution Files

All the solution files are stored on the web and so the solutions can be downloaded and viewed by anyone who has access to OPERA. The source code is also available if anyone has queries about any particular model.

To help those who don't have access to OPERA but would like to see results from the model, and to make it easier to get access to those results, an autogen script was written that took the model solution and generated many images of BMod, Vector Field Plots and Error Plots over the x, y and z planes of the model at 1 m and 2 m spacing (axis dependent). These plots are then posted onto the modelling website and can be accessed directly.

2.7 Vector Fields Consultancy

To give us some confidence in the Hall model we approached Vector Fields and asked them to validate the hall model; we also asked for some advice on specific issues relating to using the hall model as a basis for sub-modelling.

These reports have now been published and are available on the modelling website at

http://www.hep.shef.ac.uk/research/mice/opera_models/

Vector field produced two reports, the first deals with the hall model itself whilst the second deals with issues surrounding sub-modelling and how that would integrate with the hall model. In this section the conclusions from the reports will be outlined but for further details the reader is refered to the reports themselves.

2.7.1 Report1: Validation and Improvement Suggestions for MICE Experimental Hall Modelling

For this report VF used model 91 which was step IV 240 MeV/c solenoid mode. Enough information was given in the reports on the process that they undertook that it would be possible to independently repeat the validation for the other models if this was deemed necessary. However as we are primarily concerned with Step IV this step has not been taken and will not be pursued further here.

In this report Vector Fields looked at five items which will be briefly overviewed.

Item 1 - Comparison of fields in free space

By comparing of a couple of line integrals and a patch on a model with all the elements set to air with Biot Savart Calculations it was determined that the error on those compared areas was less than or equal to 0.21%. This is indicative of the error introduced by the finite mesh.

As the lines/patch do not represent the entire model the error in any given region may be more or less than this but it is understood that this is indicative that the meshing of the model is adequate.

Item 2 - Adding ferromagnetic components to the model

In this study the ferromagnetic components were grouped into six groups that were spatially/functionally related. A model was run with all components set to air and then successive models were run with each group of components having its native BH curve switched on. For each model the effect on the three patches defined in item 1 was looked at.

Once again the location of the patches has an influence on the results of the study and so care must be taken in interpreting the results for other areas, particularly if the area of interest is likely to be near a ferromagnetic object.

There were two results from this study which are copied verbatim from the report:

'This investigation shows that the most significant components are those which substantially affect the return path of the flux. While the results presented have been necessarily reduced, they are representative of important areas in the model where sensitive equipment is potentially to be mounted.

The models produced for these studies can be used for field recovery in any other area of the meshed space.'

'It is probable that the MICE Hall model already contains enough of the significant components for the fields in free space to be accurate within 1 or 2% - remembering of course that all fields may be at least 0.2% of the 'all free space' value in error anyway. From Cobham's knowledge of the MICE Experimental Hall, there do not appear to be any major components that have been omitted that will further significantly affect results'

Item 3 - Investigation of material property variations

In this item the magnetisation values of BH curves of the steel was reduced by 10% and the effect on the three patches defined in Item 2 was calculated. The observed changes were usually well below 5%. The reduction in the magnetisation of the shielding walls means that they are not performing quite as well but as they are generally far from saturation in model 91 the effect is quite small.

The conclusion was that the uncertainty about material properties in the structures should only be of a minor concern. Note however that this result only applies to the step IV models.

Item 4 - Investigation of mesh quality

The hall model has been run using quadratic elements throughout as this is the safest and most accurate method of calculating the fields. Unfortunately quadratic elements impose a heavy cost in terms of the number of equations that need to be solved, hence increasing both the size and solve time of the model. To investigate whether the use of quadratic elements was necessary two models were run, one with mixed elements and one with all linear elements. The integrated fields on the patches were compared with the results from the quadratic model.

The results showed that on the patches examined the benefit of using quadratic elements was marginal yet the solve time improvement was significant.

Care needs to be taken in switching to running models with linear elements. The quadratic elements are of use where the field gradient is high or where high accuracy is sought. So for the general solution where the solution file

could be taken by anyone to ascertain the field anywhere in the model a quadratic solution is the safest although a mixed solution may be ok.

This result could be of much use for speeding up the process for finding fields for sub-models though - see report 2

Item 5 - Substructure modelling in model 91

This final item considered using field values from the MICE Hall as a source field for a more detailed sub-structure model.

A comparison was made between running the hall model with a model of a rack in situ and using the hall model without a rack in situ but extracting a source field from the hall model and using these fields as a source for a sub model that contained the rack.

The integral of the field over a patch was examined. The results from this showed that there was a significant difference between the integral on the patch from these two approaches and this leads to the conclusion that:

'The field from an overall model not containing that substructure should not be used as a driving field for a detailed sub-model of the substructure.'

This has significant implications for any sub modelling effort.

2.7.2 Report 2: A Further Investigation of Sub-Structure and Simplification Modelling for the RAL MICE Hall

The following has been copied verbatim from the introduction of the report:

'As shown in the report on Validation and Improvement Suggestions for MICE Experimental Hall Modelling, omitting substructure from the model altogether is not valid when the source fields are obtained. However, a simplified model of the substructure can be included. In this report, different options for simplified substructure models are investigated and some indications of probable error associated with the simplification are obtained.'

A lot of this report goes into details about how to implement substructure models and will not be repeated here. However there are a number of recommendations in the report that are worth repeating. These too have been copied verbatim from the reports.

Recommendation 1 for MICE Hall model:

The effect of solving the magnetic fields in free space using a truncated finite element mesh appears to give about an average 5% error in the 'far field' in the test model. The error will be smaller closer to the solenoid coils and larger near the boundary of the model. This inherent error from using finite elements should be considered when making judgements about maximum flux density levels in critical areas of the MICE Hall by repeating this type of calculation for the complete MICE Hall model and investigating the error in the volume where a substructure model is required.

Our comment:

This follows on from the comments made in report 1 that the errors had only been calculated on specific patches and so each individual situation needs consideration.

Recommendation 2 for MICE Hall model:

Structure inside the MICE Hall that consists of a steel outer 'cabinet' with internal ferromagnetic structure can be adequately simplified to either a hollow structure of approximately the same dimensions as the outer cabinet, or an approximate cabinet with a single, appropriately dimensioned, ferromagnetic block placed at its centre. If the existing model includes structure where the block is already in place, don't bother to remove it. But, if future cabinets are added, the outer cabinet should be sufficient to get source fields for a detailed substructure model.

Recommendation 3 for MICE Hall model: Element size in the free space surrounding a substructure should not need to be reduced to the level that may be needed for a detailed substructure model in order to adequately capture the source field from the complete MICE Hall model.

Recommendation 4 for MICE Hall model:

When trying to examine the shielding effect supplied by magnetic walls, the outer boundary of the model should be made as large as practically possible to avoid image sources.

Recommendation 5 for MICE Hall model:

If substructure modelling of shielding walls is undertaken, the discretization of the wall and supports only needs to be at a reasonable level to capture the geometry. A fine mesh is not needed to capture variations in flux density as these will be small.

Recommendation 6 for MICE Hall model:

A quick way to assess how effective shielding will be whether it is real shielding constructed for the purpose of reducing field or the outside cabinet of some equipment is to determine where the steel is operating on the magnetic characteristic of the shielding material. Tangential components of magnetic field strength and the normal component of magnetic flux density will be continuous at the material surface, so this will also give an indication of the flux density just behind (or inside) the shielding wall.

Recommendation 7 for MICE Hall model:

Simplified models of the shielding walls in the model should be adequate to determine if the flux density is low enough for equipment to be mounted behind them, unless the sensitive equipment is very close to discontinuities in the wall occurring because it is constructed from a finite number of plates. Substructure modelling will not be beneficial. An assessment of the error in the source field associated with the finite element representation should be made in the same vicinity to determine whether the reduction of the field due to the shielding can be considered accurate.

Conclusions from the 2nd report

1. The effect of the meshing and truncation of infinite space should be assessed in any area where it is important to determine if sensitive equipment can be mounted. This should be achieved by comparing Biot-Savart calculated fields with fields recovered from the mesh assuming all materials have free-space permeability

2. Detailed substructure models can use the overall MICE Hall model to derive a source field providing: a. There is a simplified representation of the steel container and its contents included in the MICE Hall model b.

The differences in the source field from the solenoids caused by using finite elements compared with Biot-Savart is not larger than the source field values for the sub-structure

3. Hollow tanks, or tanks with an equivalent centralized volume of magnetic material offer a better approximation than tanks completely filled with a dilute magnetic material.

4. It is not accurate to extract the source field for a substructure model from a model of the MICE Hall that does not include a simple representation of the structure - see the earlier results obtained in the other MICE Hall report for including the rack in Model 91.

5. Substructure modelling behind shielding walls should not be necessary unless the sensitive equipment is placed very close to discontinuities in the wall. The differences in source field associated with truncation of the mesh will probably be larger than the error introduced by simplification.

3 Baseline Magnetic Mitigation Scheme

3.1 Overview

3.1.1 Introduction

This section details how the Mice Hall Model has been used to give an overview of the stray fields likely to be observed in the MICE hall and the surrounding areas.

To start this section it was through that it would be useful to provide the reader with a set of overview and reference plots of the predicted field level throughout the entire volume of the hall model at beam height for both solenoid and flip mode at step IV (240 MeV/c) - see figures 5 to 8. Of course at this scale a lot of detail is lost; we will return to areas of detail later.

All of these plots are plotted on a five gauss scale. Note that where the field is >5 gauss the field is not plotted, so either details of structures behind the plot can be seen more clearly, or where there are no structures a white background can be observed.

All of the 2D plots are produced using Nodal interpolation with integral fields. This may be slightly less accurate than using a full integration method but given the number of elements in the hall model the full integration method will not produce 2D plots in a tractable time. As alluded to earlier Vector Fields demonstrated that the mesh on a test patch within the hall volume was accurate to <1%. It is likely that that the error will increase as one moves towards the edge of the model as the mesh size increases, however as this is a larger error on a very small field value this is of no significance.

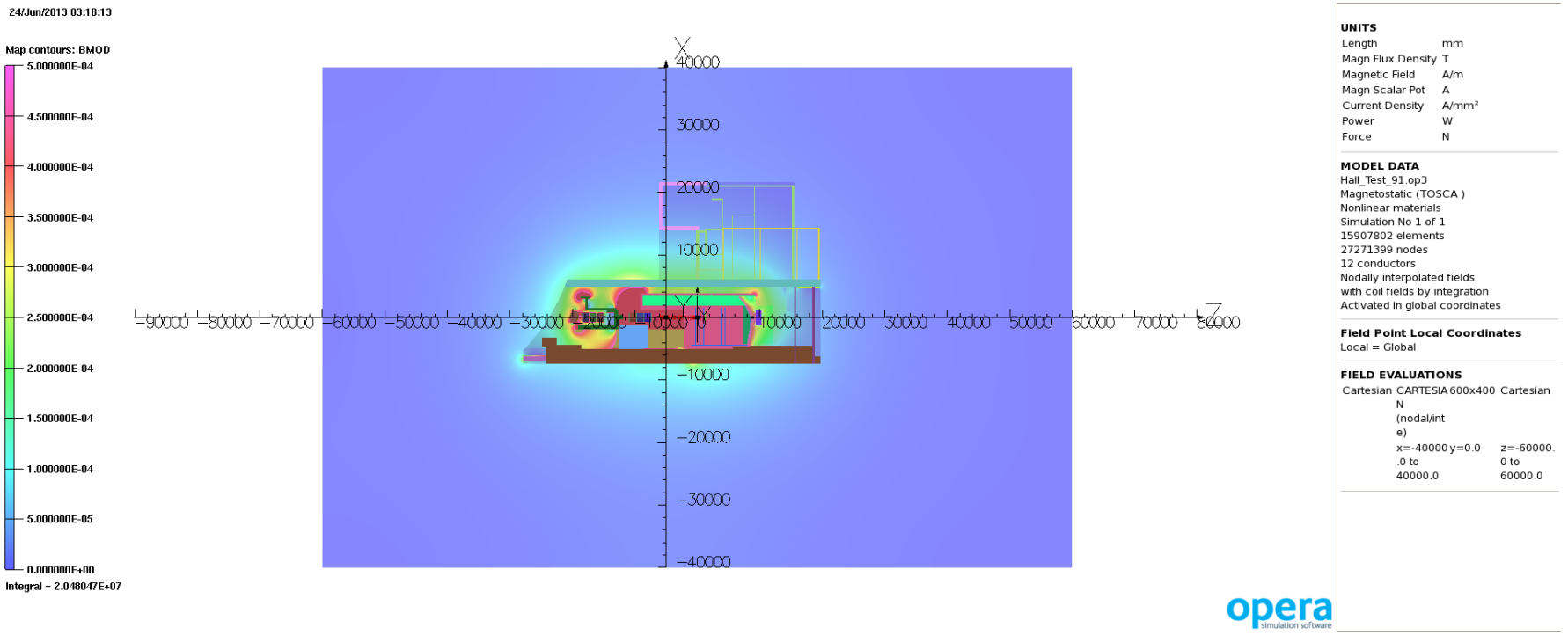

Figure 5: Bmod 5 gauss scale. Step IV 240 Mev/c Solenoid Mode. Overview of Model Volume at Beam Height from Model 91. The Model is shown with structures turned on. One can immediately see that the majority of the stray field is contained within the MICE hall.

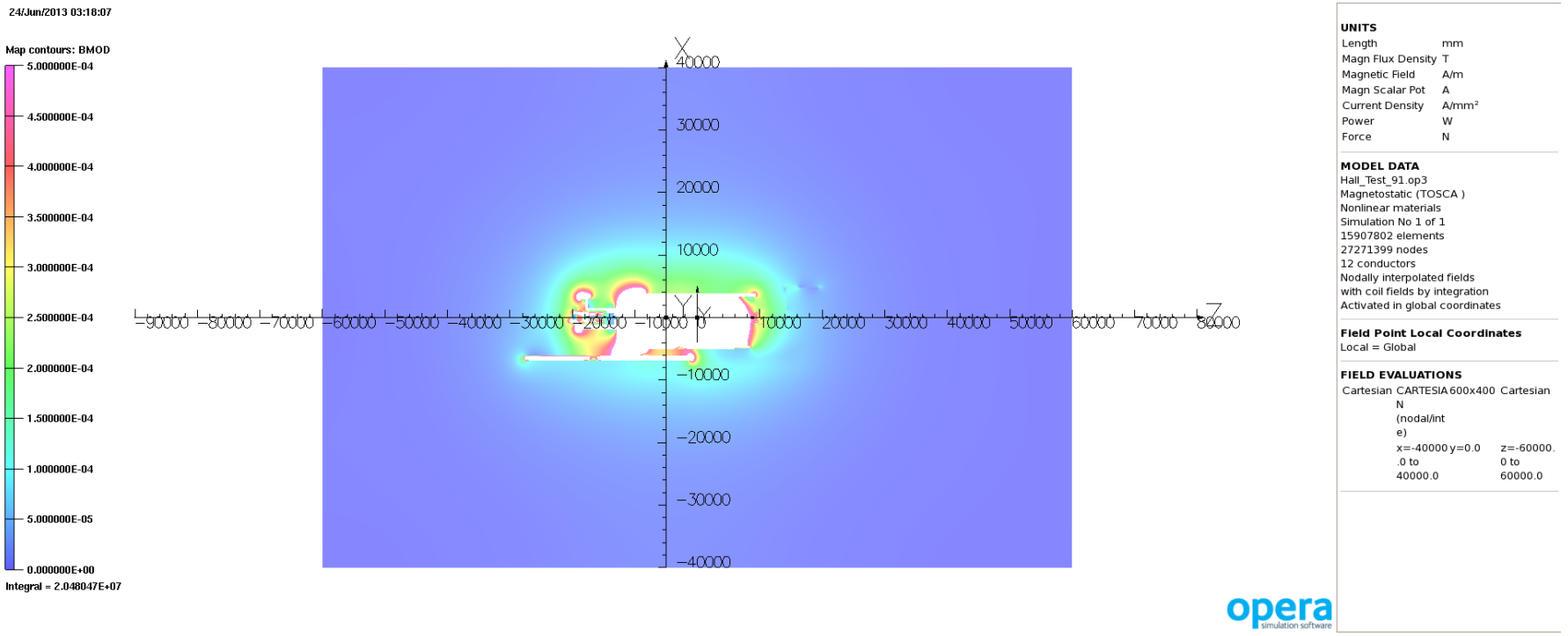

Figure 6: Bmod 5 gauss scale. Step IV 240 Mev/c Solenoid Mode. Overview of Model Volume at Beam Height from Model 91. The Model is shown with structures turned off.

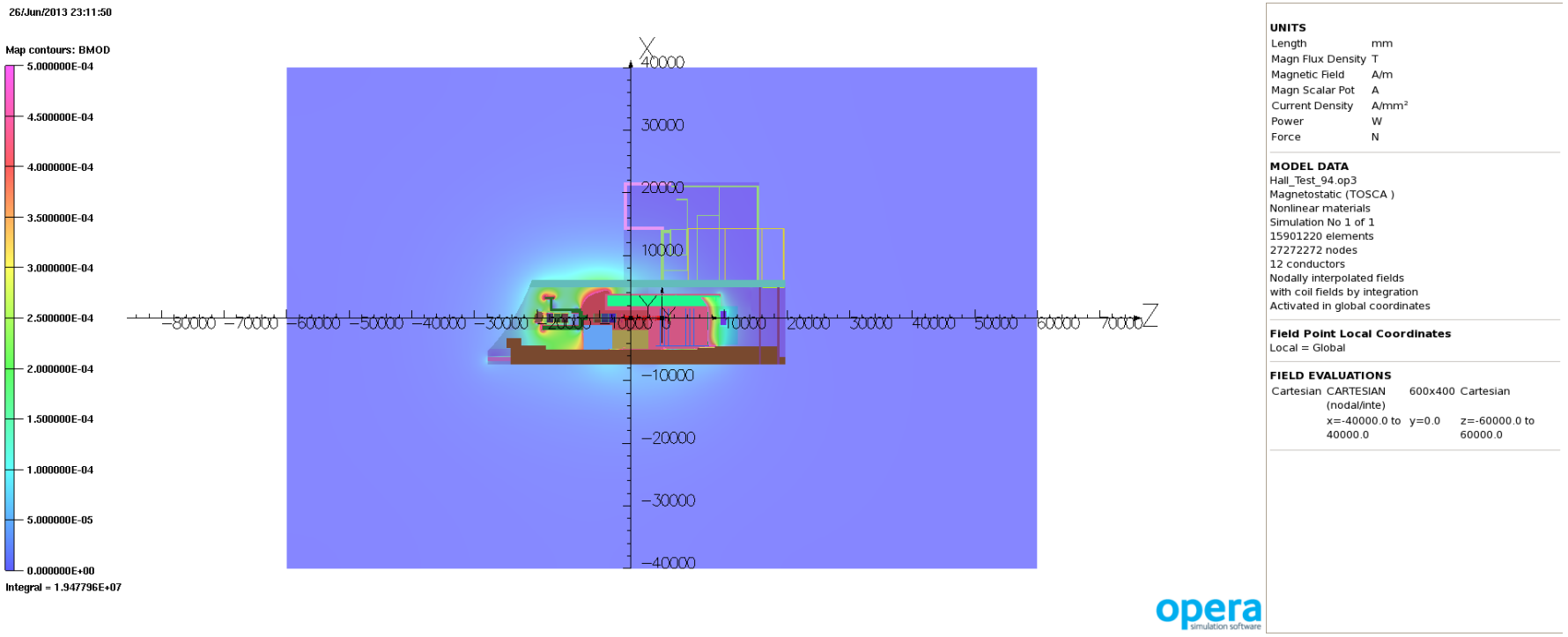

Figure 7: Bmod 5 gauss scale. Step IV 240 Mev/c Flip Mode. Overview of Model Volume at Beam Height from Model 94. The Model is shown with structures turned on. One can immediately see that the majority of the stray field is contained within the MICE hall.

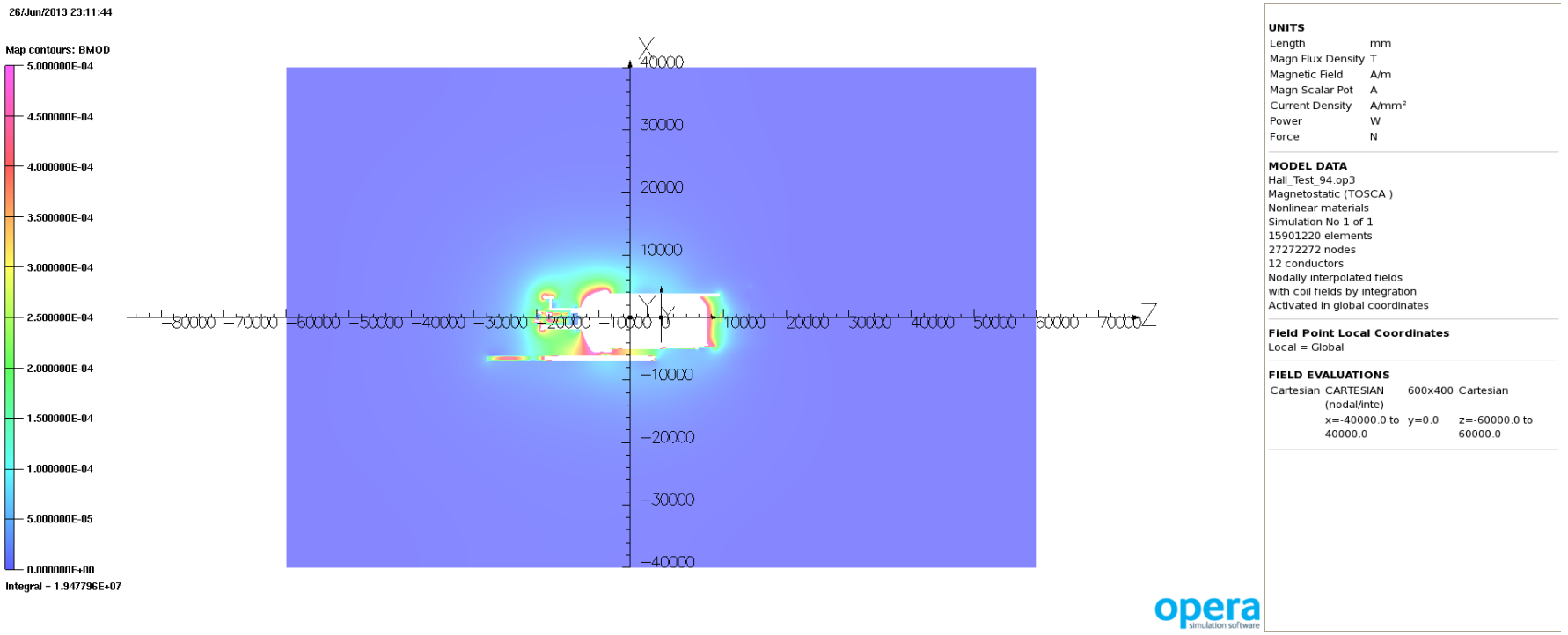

Figure 8: Bmod 5 gauss scale. Step IV 240 MeV/c Flip Mode. Overview of Model Volume at Beam Height from Model 94. The Model is shown with structures turned off.

3.1.2 Field Outside of the MICE Hall

The plots in this section show the maximum observable field calculated on the external faces of the MICE Hall walls/roof/floor. The images shown are for Step IV solenoid mode only as this mode of operation produces the highest external fields for step IV as there is less field cancellation in the cooling channel. No images have been shown for the East wall but this is far enough away not to be of concern.

The only area external to the MICE hall that indicates that there may be fields above 5 gauss is on the roof. As these are simulated predictions it is clear that once the magnets are installed, then field measurements would need to be taken to establish the validity of these particular simulation results. It is understood that public access to areas above 5 gauss would need to be limited; as the MICE hall roof is not considered to be public access then restricted access to this area should not be a problem. The effects of any stray fields upon equipment installed on the MICE hall roof has not been established.

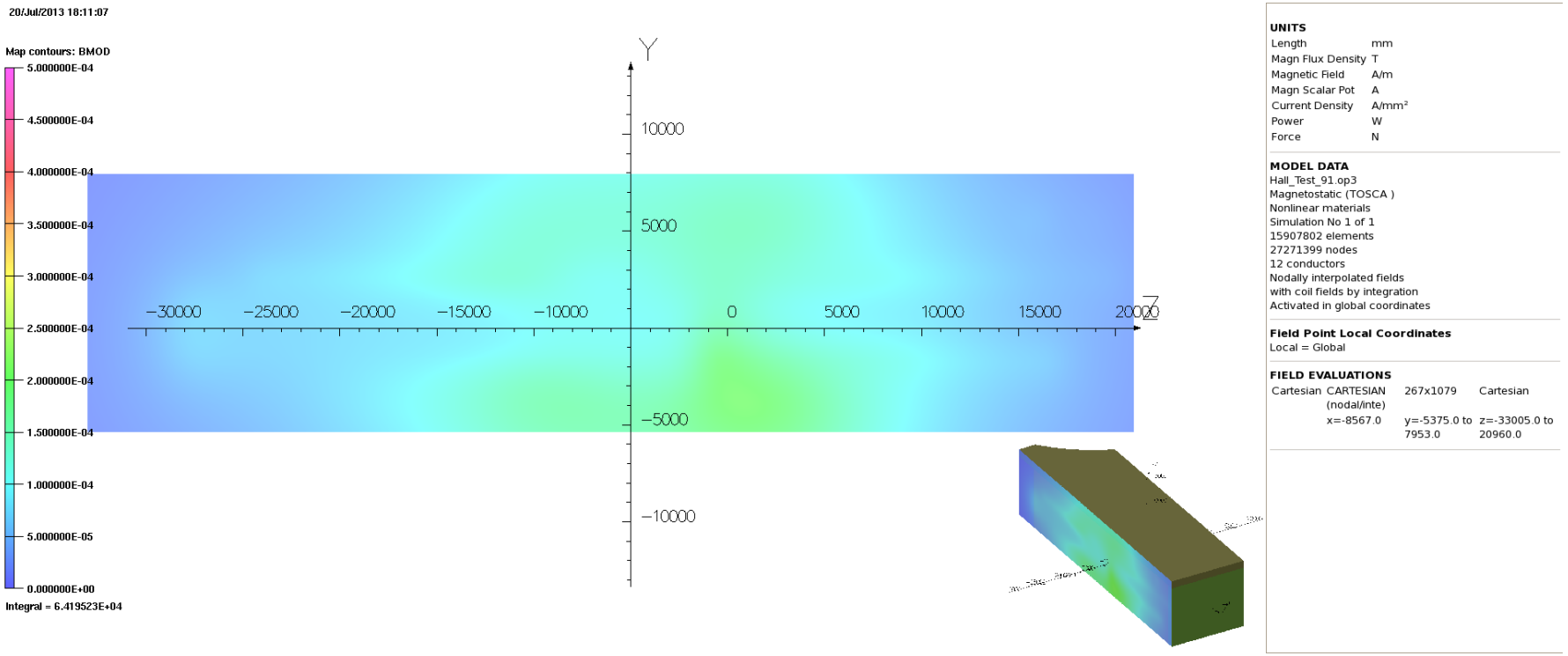

Figure 9: Bmod 5 gauss scale. Step IV 240 MeV/c Solenoid Mode. North Wall Side view.

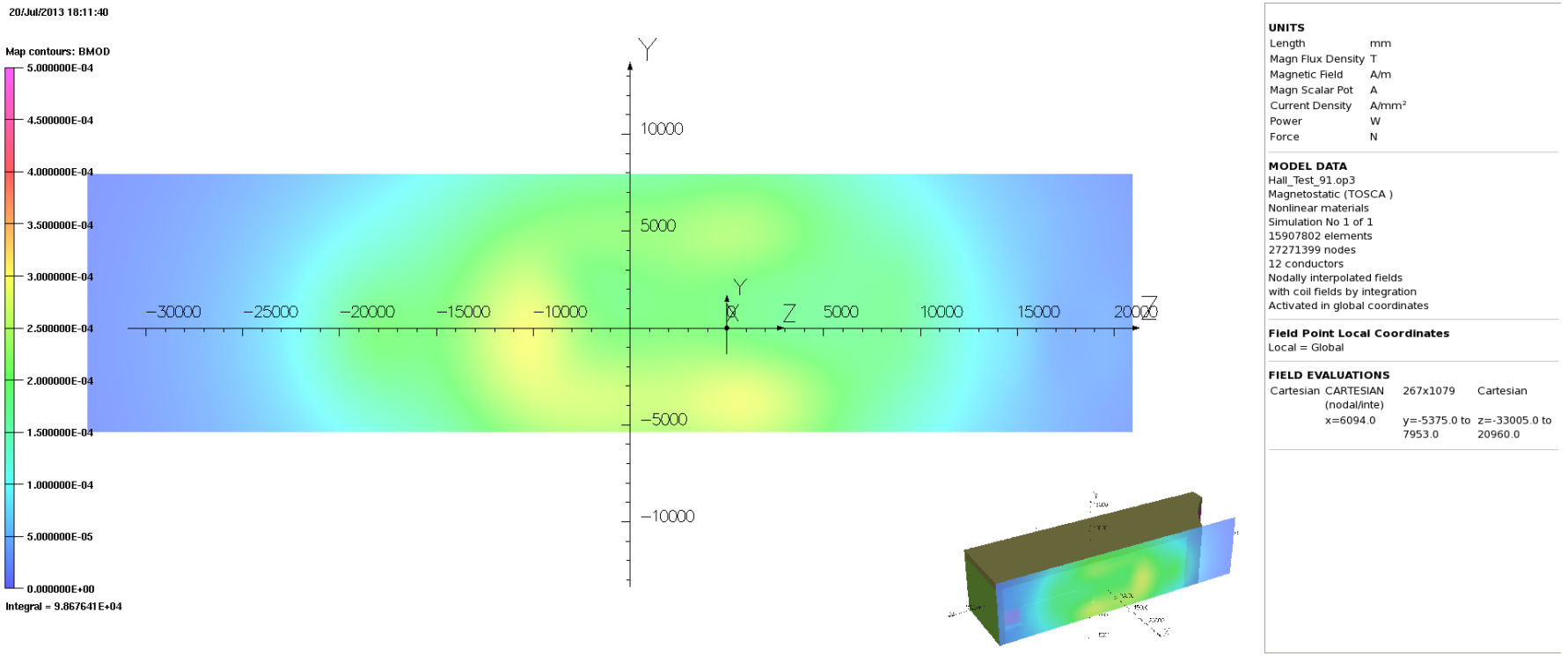

Figure 10: Bmod 5 gauss scale. Step IV 240 MeV/c Solenoid Mode. South Wall Side view.

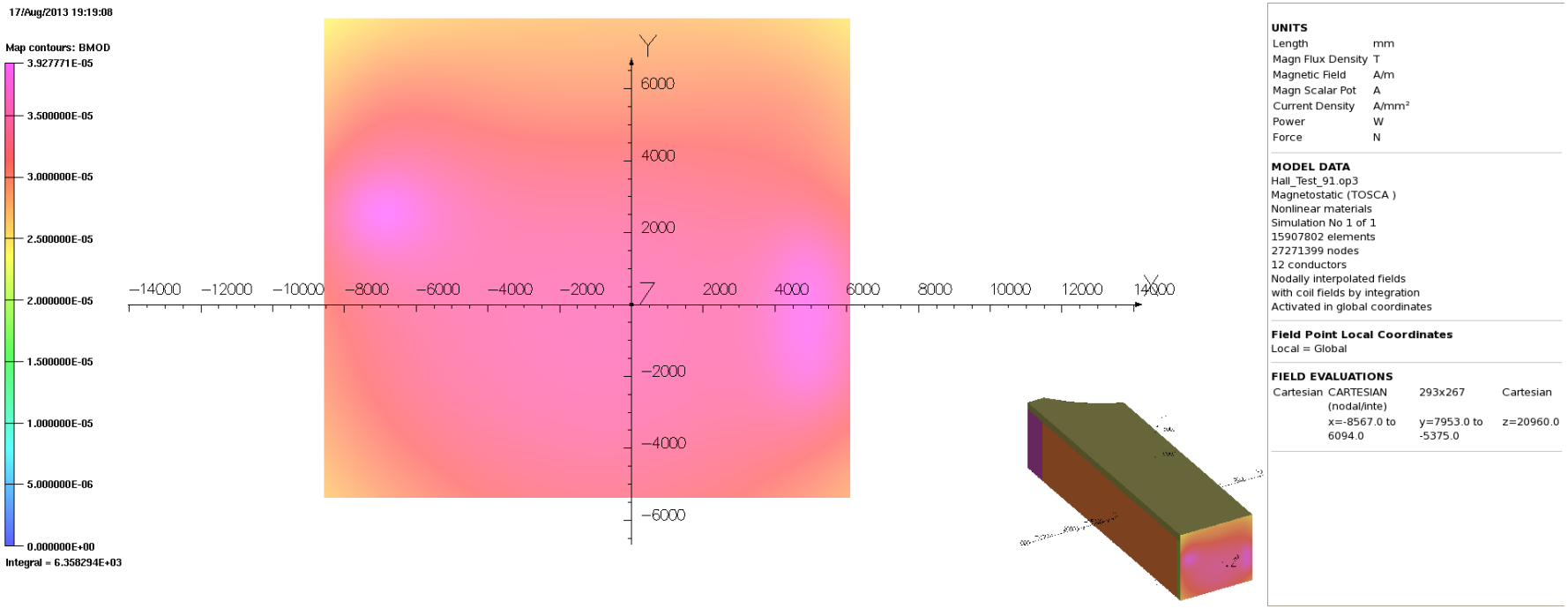

Figure 11: Bmod. Step IV 240 MeV/c Solenoid Mode. West Wall Isometric view. The predicted field is the same magnitude as that of the earth's magnetic field.

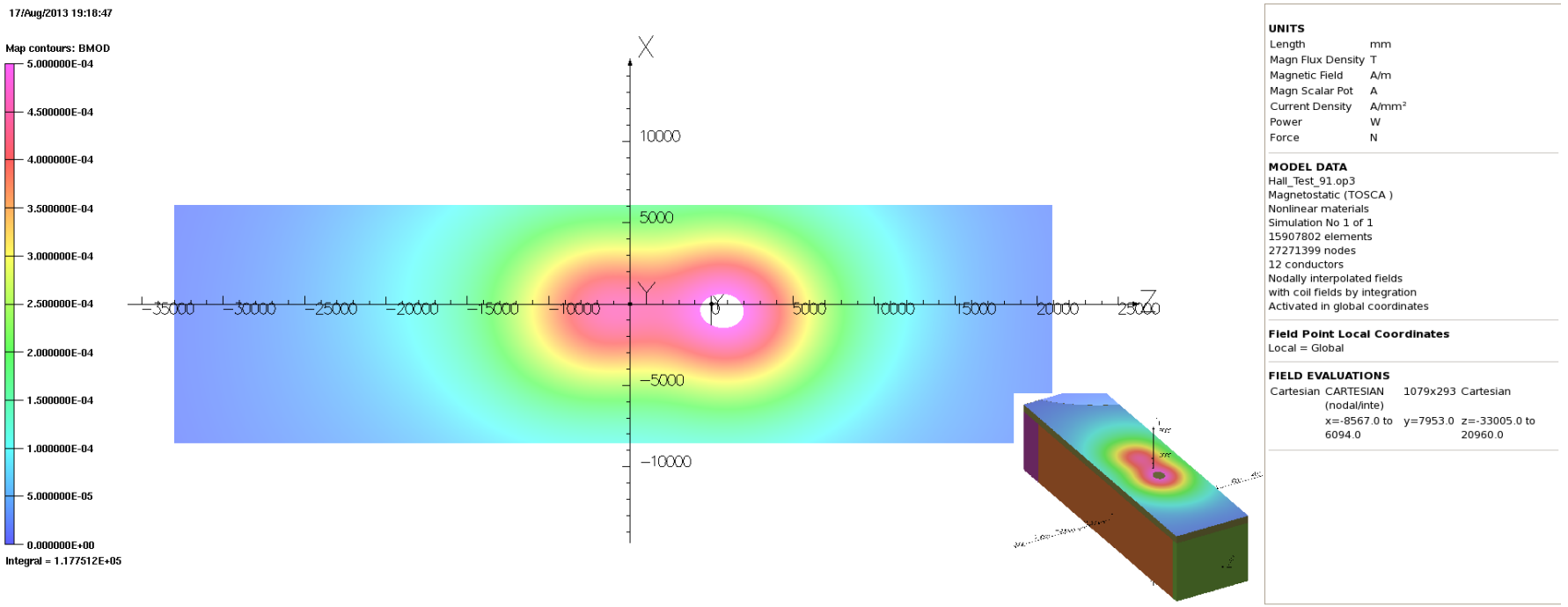

Figure 12: Bmod. Step IV 240 MeV/c Solenoid Mode. External to Roof. This is the only plot where the external field goes above 5 gauss.

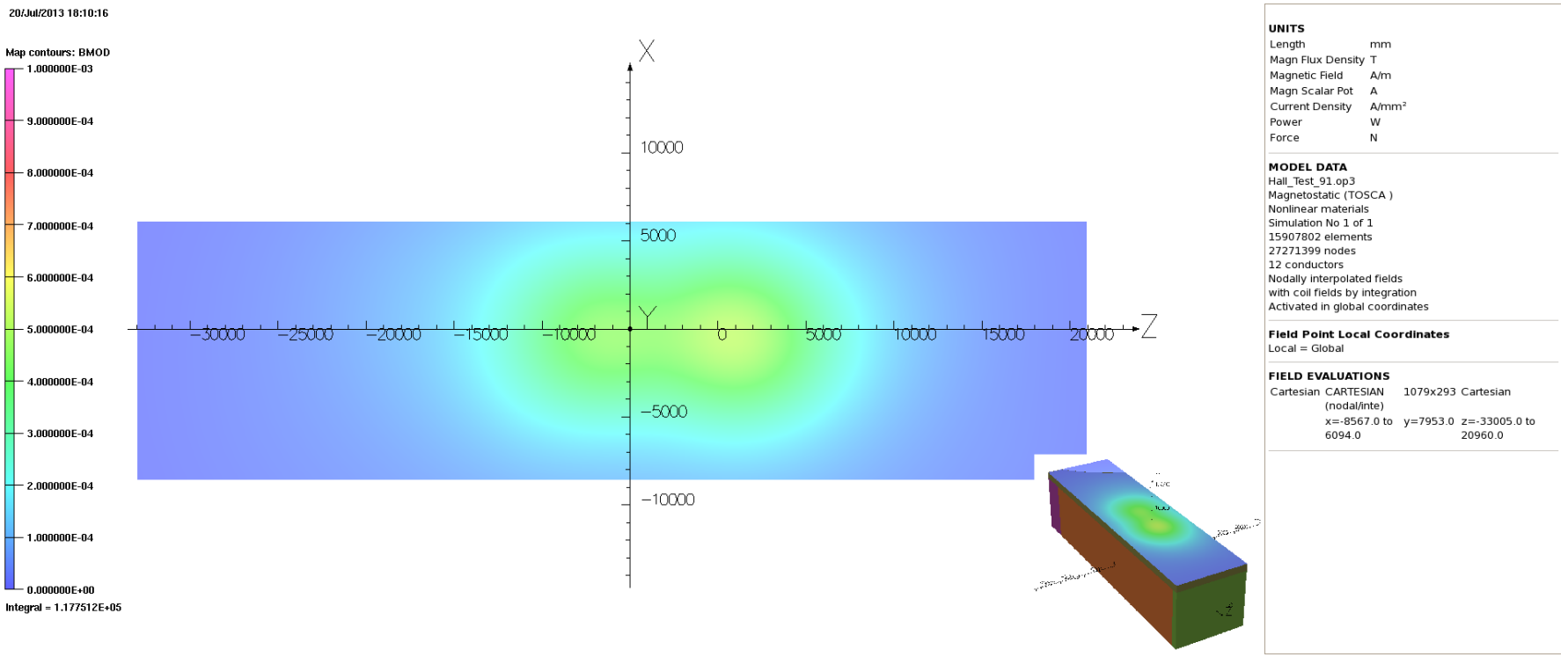

Figure 13: Bmod. Step IV 240 MeV/c Solenoid Mode. External to Roof. This is a 10 gauss plot of the roof. The peak areas are only just above 5 gauss.

3.1.3 Mice Hall West Wall

It was clear from earlier analysis that the compressors were not ideally located and that they required moving, this was discussed in section [REFERENCE TO JASON's SECTION ON THE WEST WALL MEZZANINE].

Early models of the MICE hall indicated that the West Wall of the MICE Hall was a relatively safe haven, this view has been confirmed as the hall models have been further improved. Furthermore, the path to the MICE Hall West Wall is relatively free of large iron structures so it was possible to do a Biot-Savart calculation to give a first order approximation of the expected field in this region; this also provided a double check on the FEA model. In context of the simplification the Biot-Savart results gave good agreement with the FEA model. As the moving of the compressors requires significant structural work to the MICE Hall this cross check is valuable as it is not possible to do an in-situ measurement of the field until after the fact.

Figure 14 shows a drawing of the proposed location of the compressor locations along the West Wall.

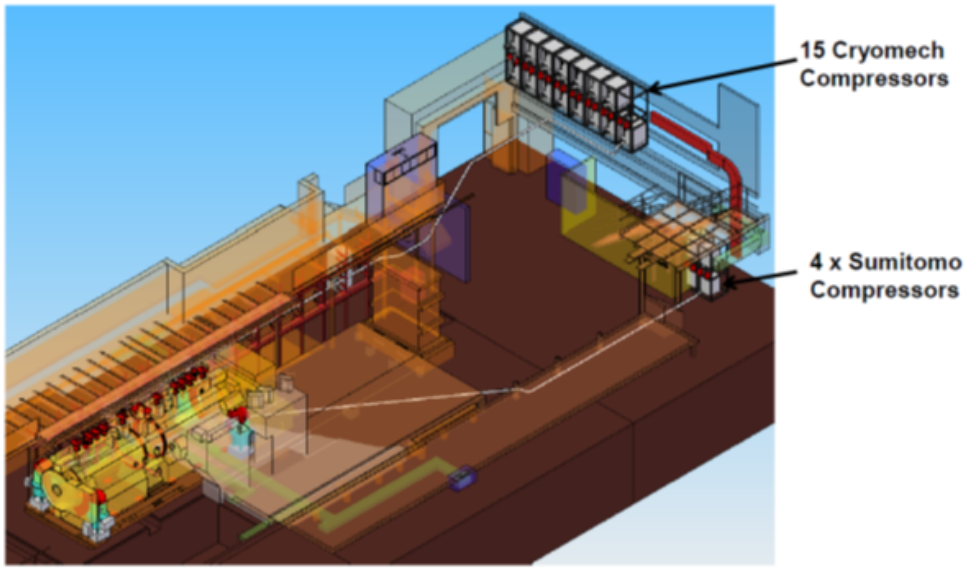

Figure 14: Location of the the Sumitomo and Cryomech compressors against the West Wall for Step IV. [***Does this need a REF to Jason's Document?***]

The Cryomech compressors have a mass of 178 kg each and the Sumitomo compressors have a mass of 96 kg each. The Cryomech compressors have a

depth of 612 mm and are set back 300 mm from the West Wall.

The Sumitomo compressors have a depth of 500 mm and the centres are offset by a distance of 2000 mm from the West Wall (West Wall situated at z=19,736 mm).

Although not insignificant the overall iron density is quite low in such an extended volume and the compressor detail means that it is difficult to include this mass representatively in the hall model in a meaningful way. To create these objects and mesh them would require a fine mesh that would make the Hall model time consuming to solve. It is likely that the effect of these iron boxes on the model would be to partially shield the inner contents and locally distort the field, however given their relative distance from the bulk of the iron in the hall it is unlikely that there is enough iron in these compressors to significantly affect the magnitude of the field in this region.[1] For this reason the iron mass of the compressors was excluded from the hall FEA model and it is acknowledged that this is a known but unquantified error in the results.

Figures 15 and 16 show the predicted field at z=17,000 mm and z=19,000 mm for Model 91

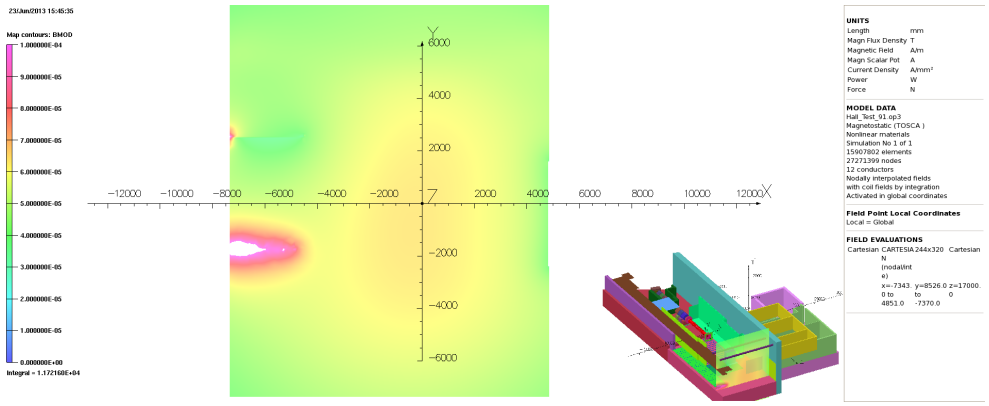

Figure 15: Bmod Field Profile towards the West end of the MICE Hall at z=17,000 mm, 1 gauss Scale. Even a couple of metres within the hall the field level is not much above the earth's magnetic field. The hot areas are where there are ferrous objects.

[1]Some earlier models were run with models of the compressors in location to try and ascertain the effect of placing this iron at the west end of the MICE hall. These models suffered from problems with meshing resolution and the results will not be presented. However it could be ascertained that the iron in these compressors did not have a significant gross effect upon the field in this region.

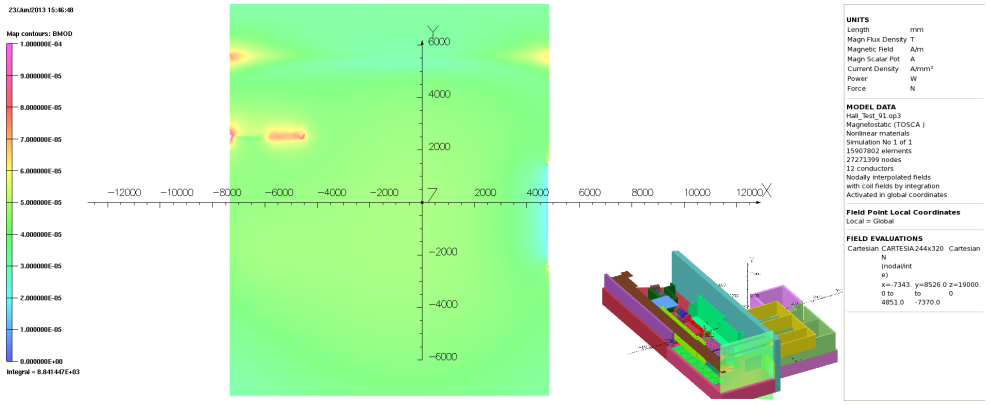

Figure 16: This is on the same scale as the previous plot but the plot is taken 2 m further away from the magnets, z=19,000 mm, close to the West Wall. (736 mm away from the wall itself.)

3.1.4 ISIS Control Rooms

The ISIS control rooms are three rooms that form part of the South Side Buildings (SSB); a nomenclature used for the model as they are on the south side of the MICE hall. These buildings, the operations room, main control room and diagnostics room are located adjacent to the MICE Hall South wall but on its upper level and are partly shielded from the MICE magnets by the South Shield Wall. The ISIS control rooms contain a significant amount of diagnostic and control equipment that is used for the operation of the ISIS accelerator. No iron mass is assumed to exist in the ISIS control rooms, although in reality there is likely to be some structural steelwork and racks.

Figure 17 shows the relative location of these rooms with respect to the the MICE hall in the MICE hall model.

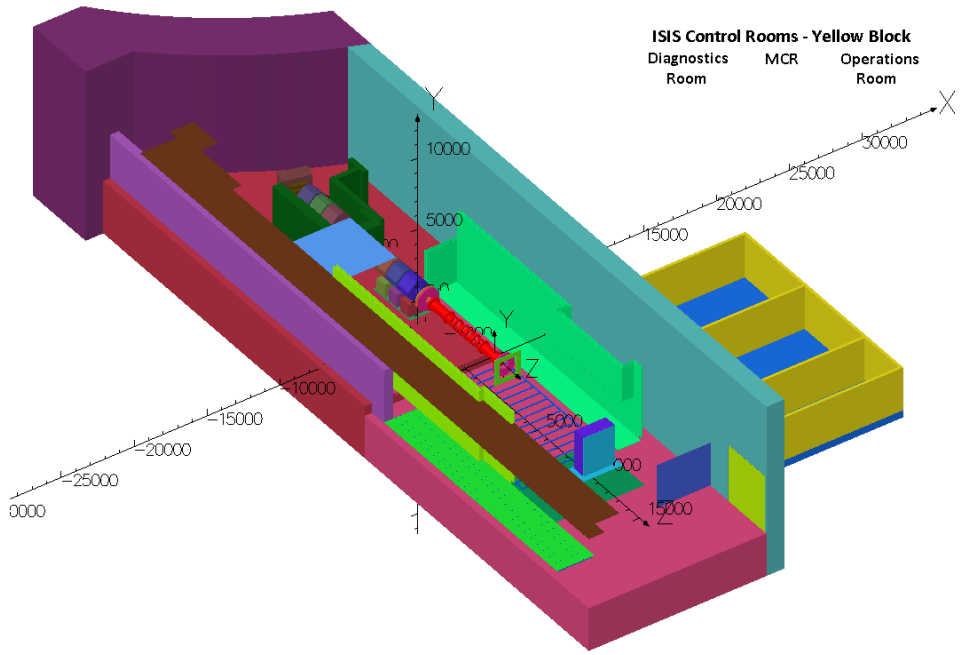

Figure 17: This shows the relative location of the ISIS control rooms to the MICE hall. The South Shield wall partially covers the diagnostics room.

Figures 19 through to 22 show the field predicted on the outer boundaries of these rooms for step IV solenoid mode 240 MeV/c.

Figure 18 shows the predicted vector field that passes at a height of y=3000 mm, this is ≈1 m above the height of the floor in the ISIS control rooms. Be aware

that there will be a component out of the plane that will be difficult to distinguish in this figure.

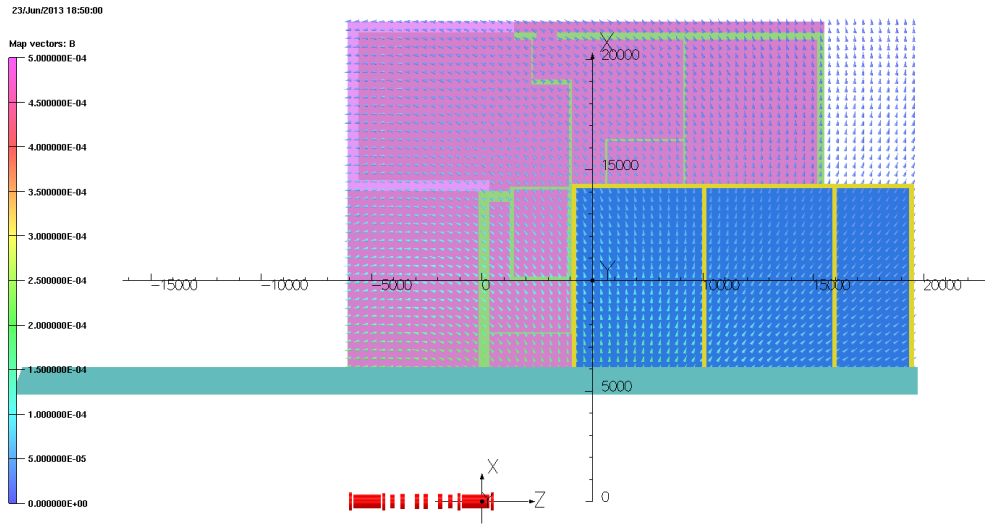

Figure 18: This shows the predicted direction of the magnetic field as it passes through the ISIS control rooms at ≈1 m above the height of the ISIS control room floor.

The reader should be aware that there is some concern that the Shield walls may not be quite as effective in reality as they are calcualted to be in the MICE Hall Models, although quantifying this is difficult. This may have an impact upon the field seen in these areas. Further information on this issue is described in section 3.2.2.

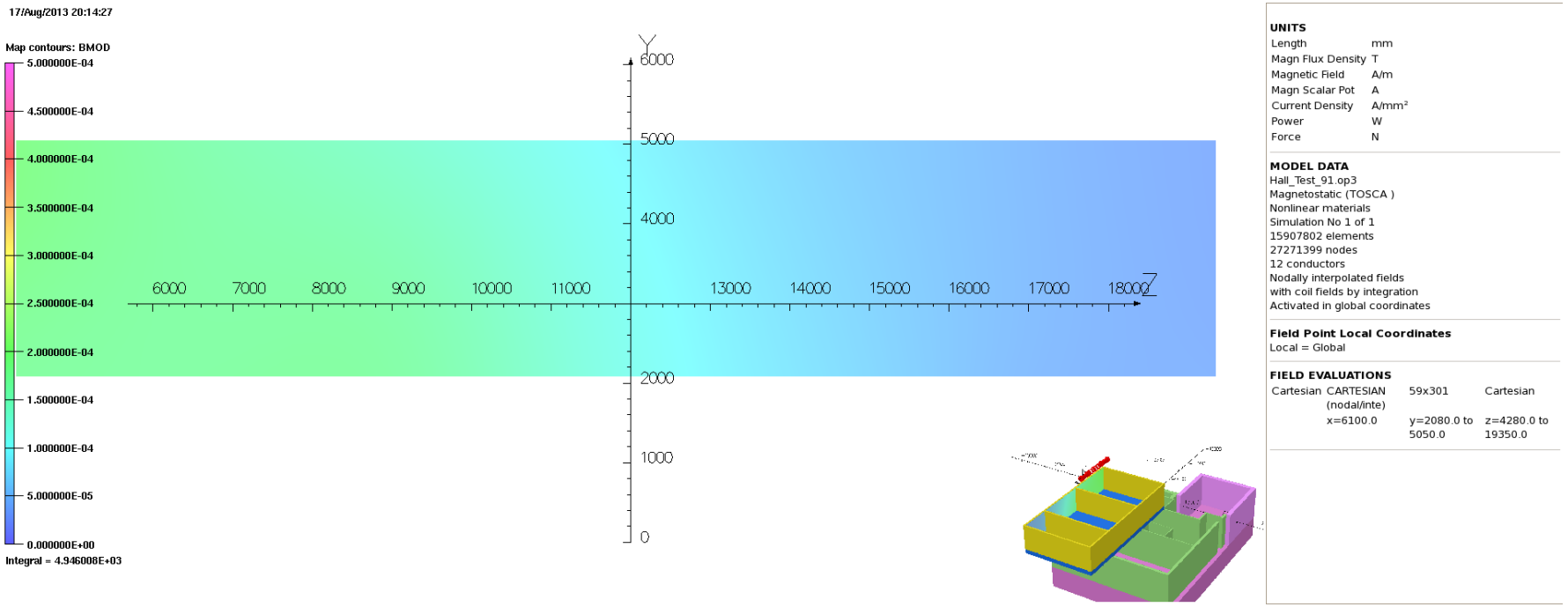

Figure 19: Bmod. Step IV 240 MeV/c Solenoid Mode. South Side of the ISIS control rooms.

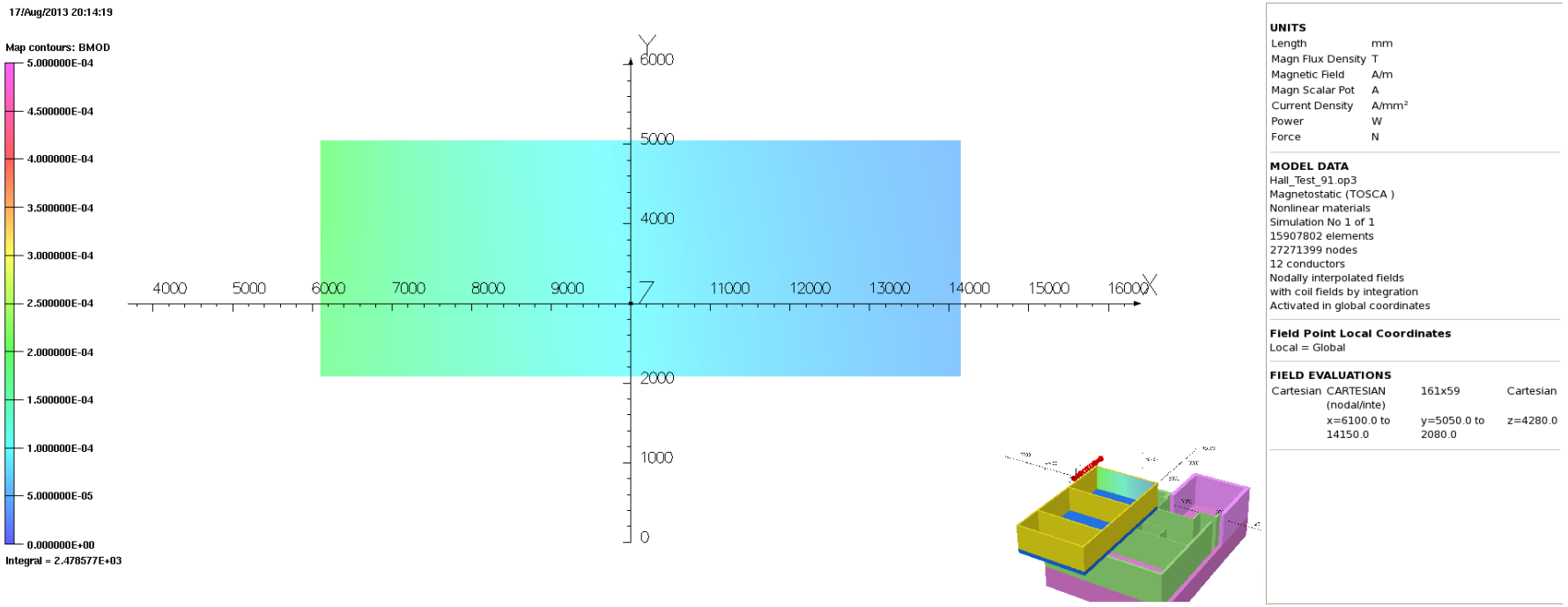

Figure 20: Bmod. Step IV 240 MeV/c Solenoid Mode. East side of the ISIS control rooms.

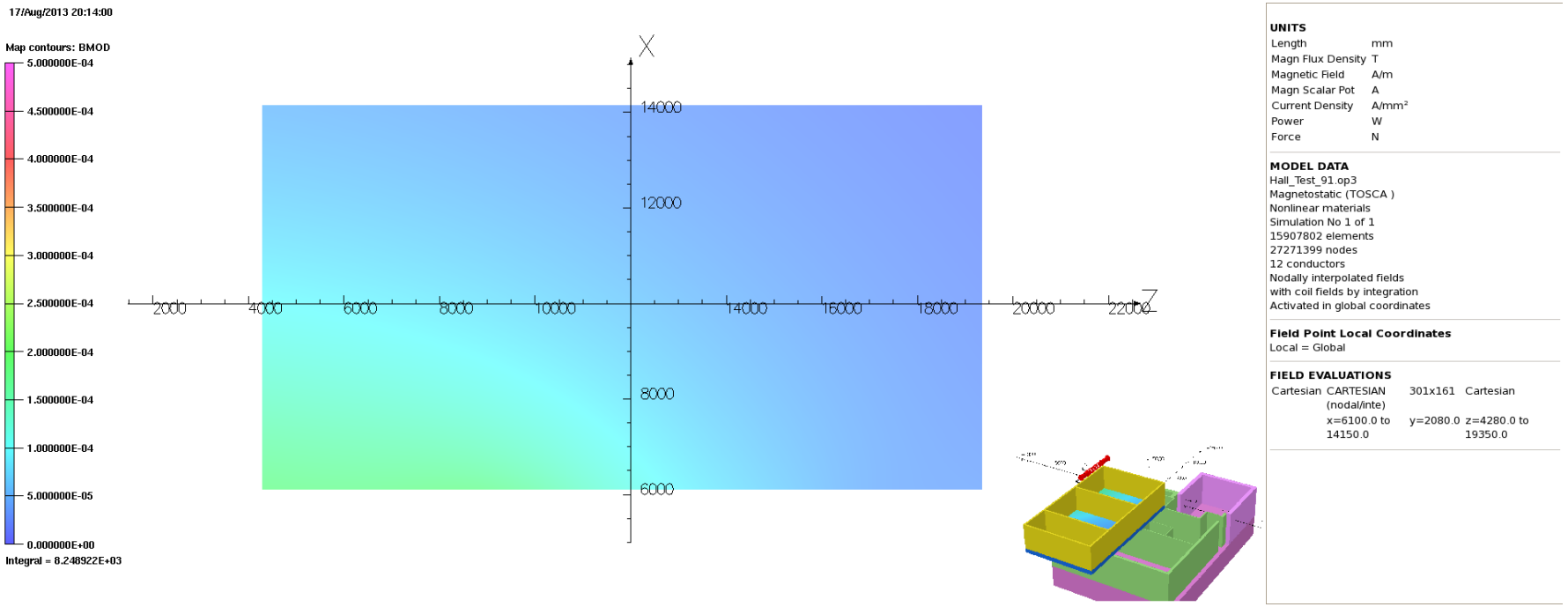

Figure 21: Bmod. Step IV 240 MeV/c Solenoid Mode. Floor of the the ISIS control rooms.

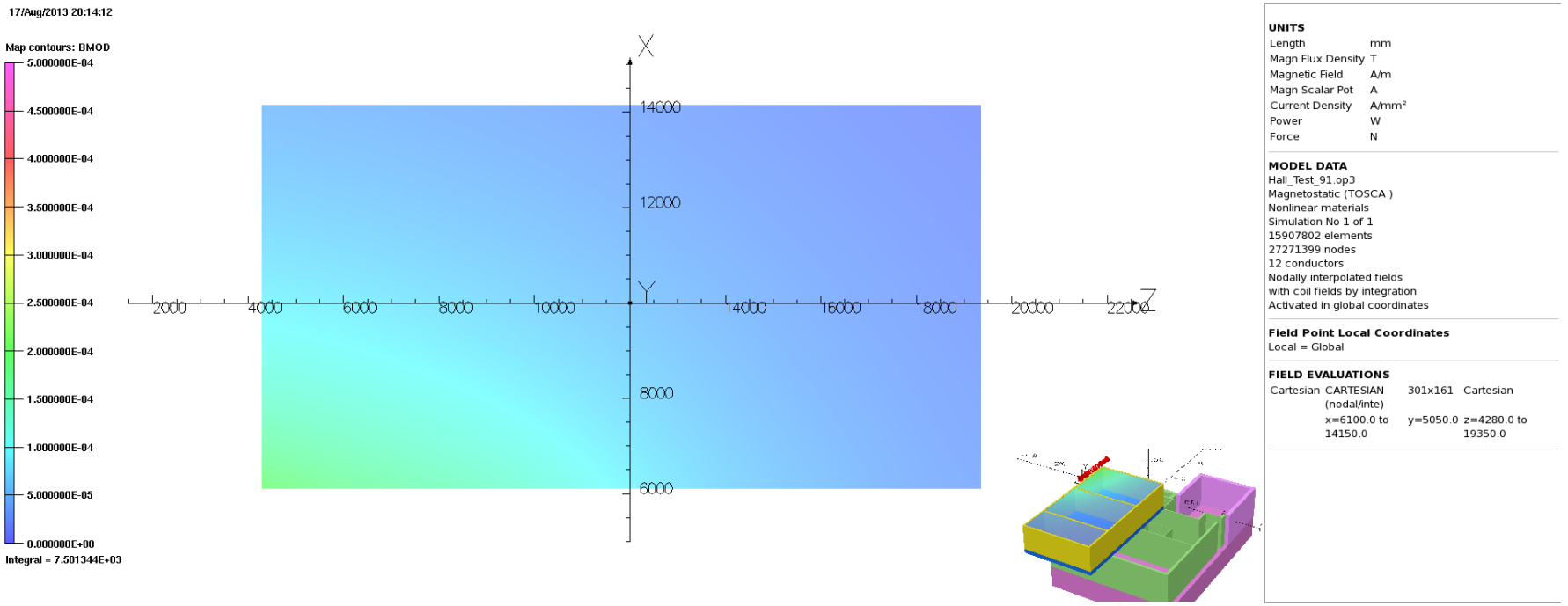

Figure 22: Bmod. Step IV 240 MeV/c Solenoid Mode. Ceiling of the the ISIS control rooms.

3.1.5 MICE Local Control Room (MLCR)

The MLCR is currently split into two sections. The section of the control room closest to the MICE hall contains much of the controls equipment and DAQ including the PPS interlock system. The section further away serves as the Control Room where the MICE staff operate the experiment from.

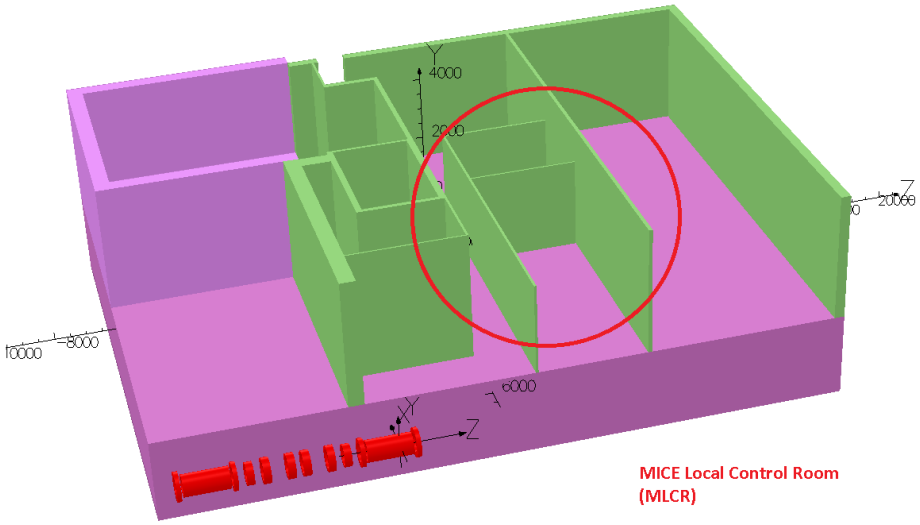

Figure 23: Location of the MLCR with respect to the MICE magnets

Figure 23 shows the location of the MLCR with respect to the MICE magnets.

Figures 25 through to 30 show the predicted field strength on the boundaries of the volume for Step IV of the experiment. These field maps were produced assuming no iron in the MLCR which is only an approximation as the racks are magnetic and so will draw some flux. The effect of this missing iron is unknown but given that the racks will represent small localised volumes of iron they are unlikely to significantly alter the field map, only localised effects would be expected. As anticipated the area closest to the hall will experience the largest air field, although typically for step IV the field doesn't appear to be much greater than ≈2.5 gauss.

Figure 24 shows a vector field map through the plane of the MLCR at x=-1000 mm. Both the field gradient through the MLCR volume and the direction of the imposed field can be inferred from this.

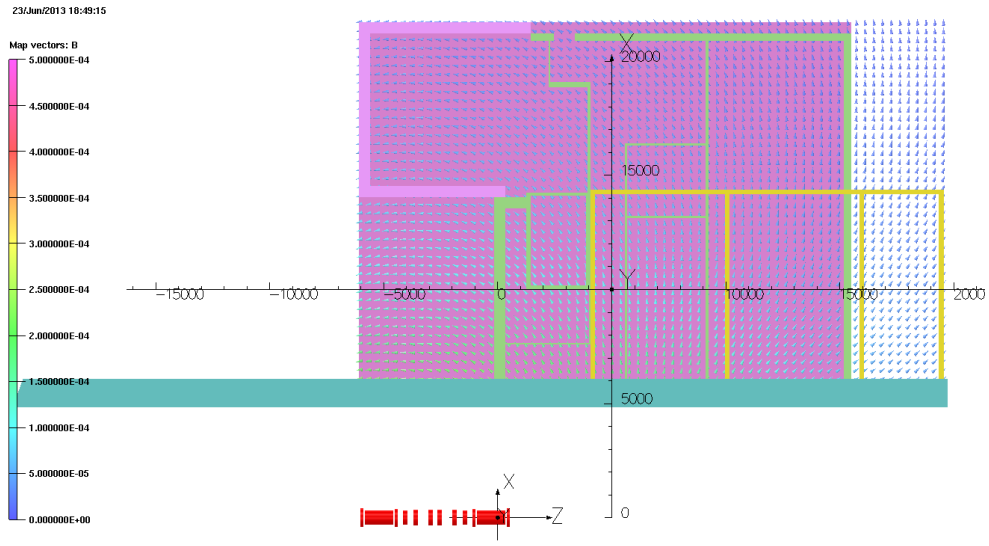

Figure 24: Vector Field map through the MLCR and surrounding buildings at a height of ≈1.3 m below the ceiling of the MLCR. Note that the yellow walls are the outline of the ISIS control room walls as seen from above.

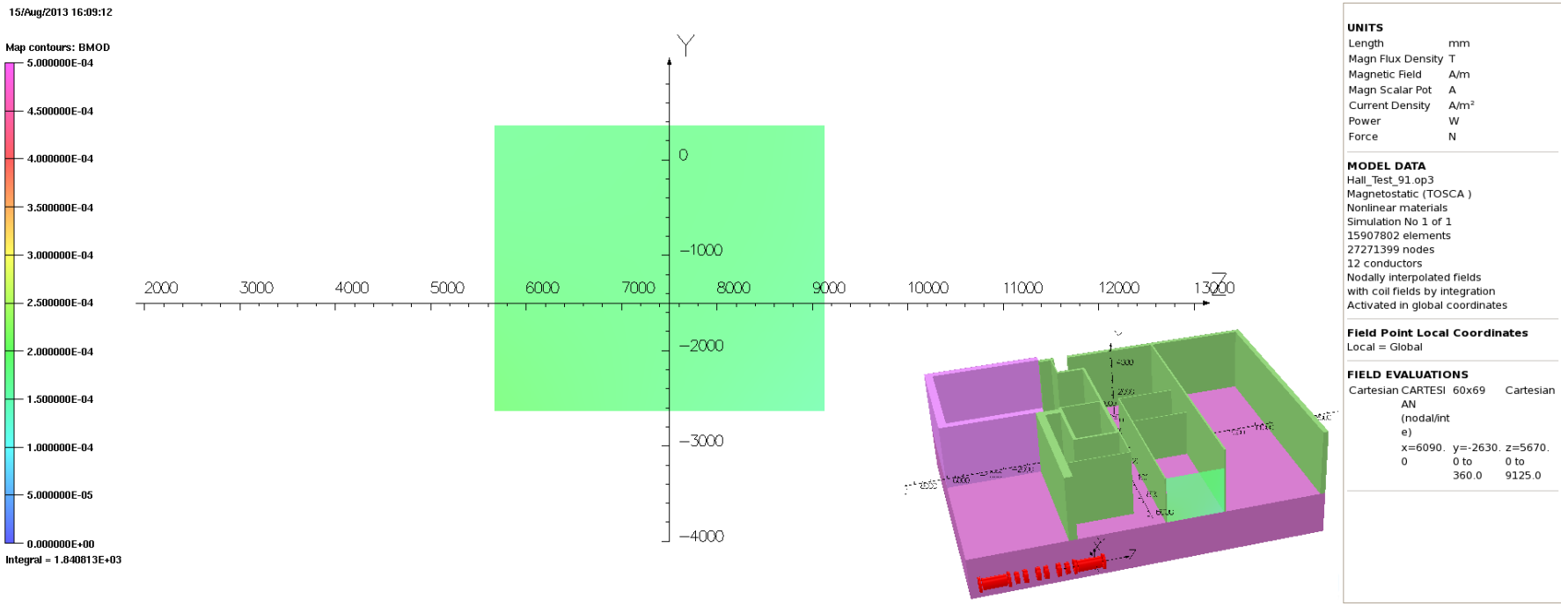

Figure 25: Bmod. Step IV 240 MeV/c Solenoid Mode. MLCR North Side.

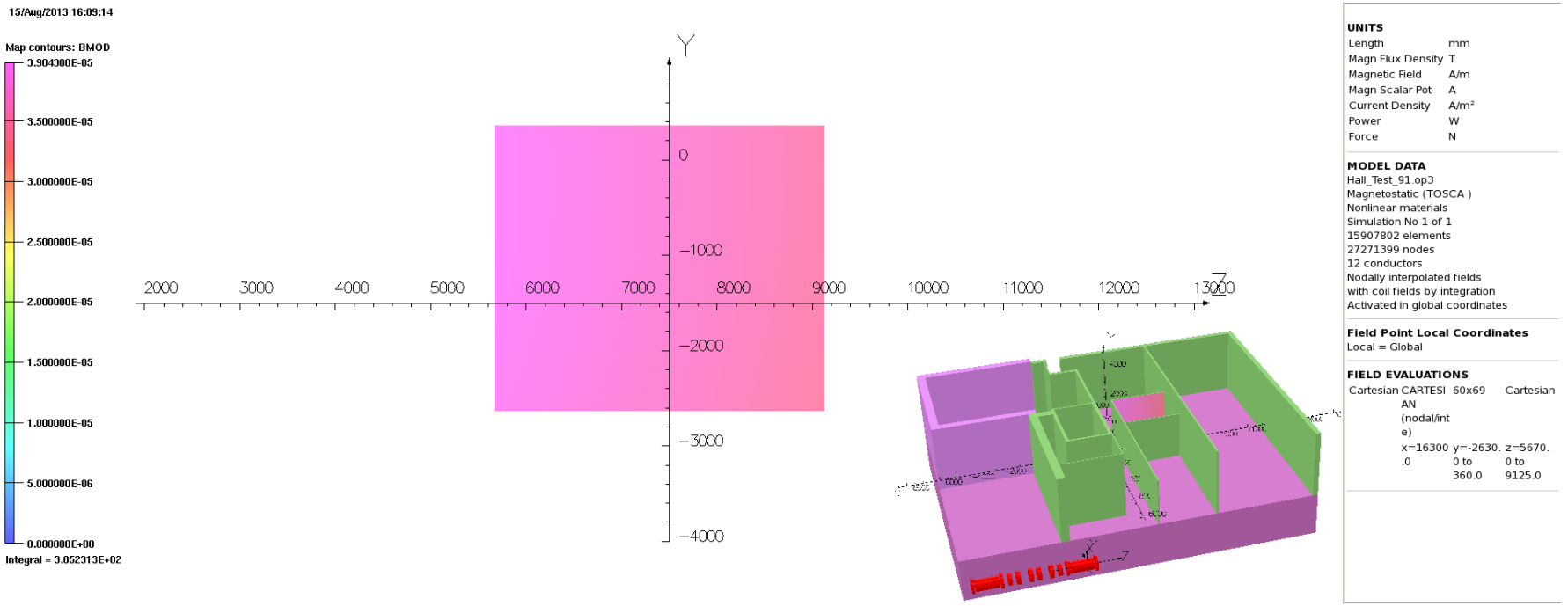

Figure 26: Bmod. Step IV 240 MeV/c Solenoid Mode. MLCR South Side. Note the different scale on this plot!

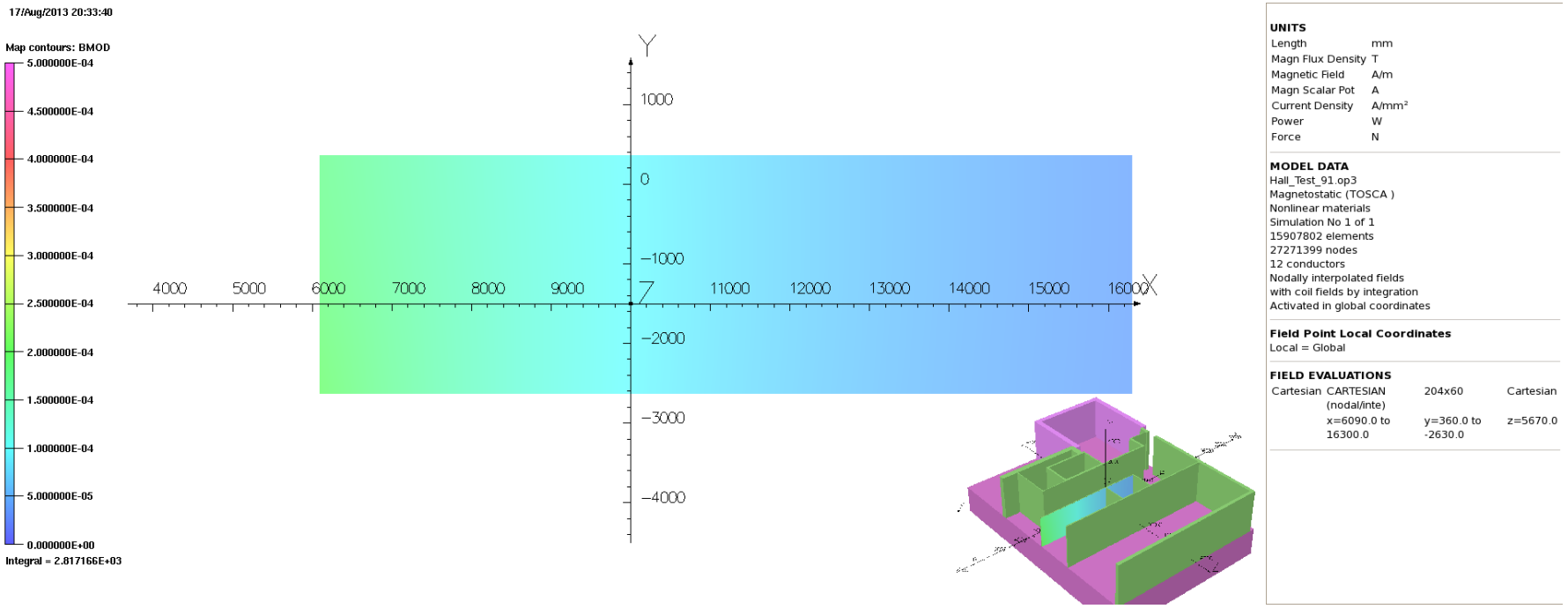

Figure 27: Bmod. Step IV 240 MeV/c Solenoid Mode. MLCR East Side.

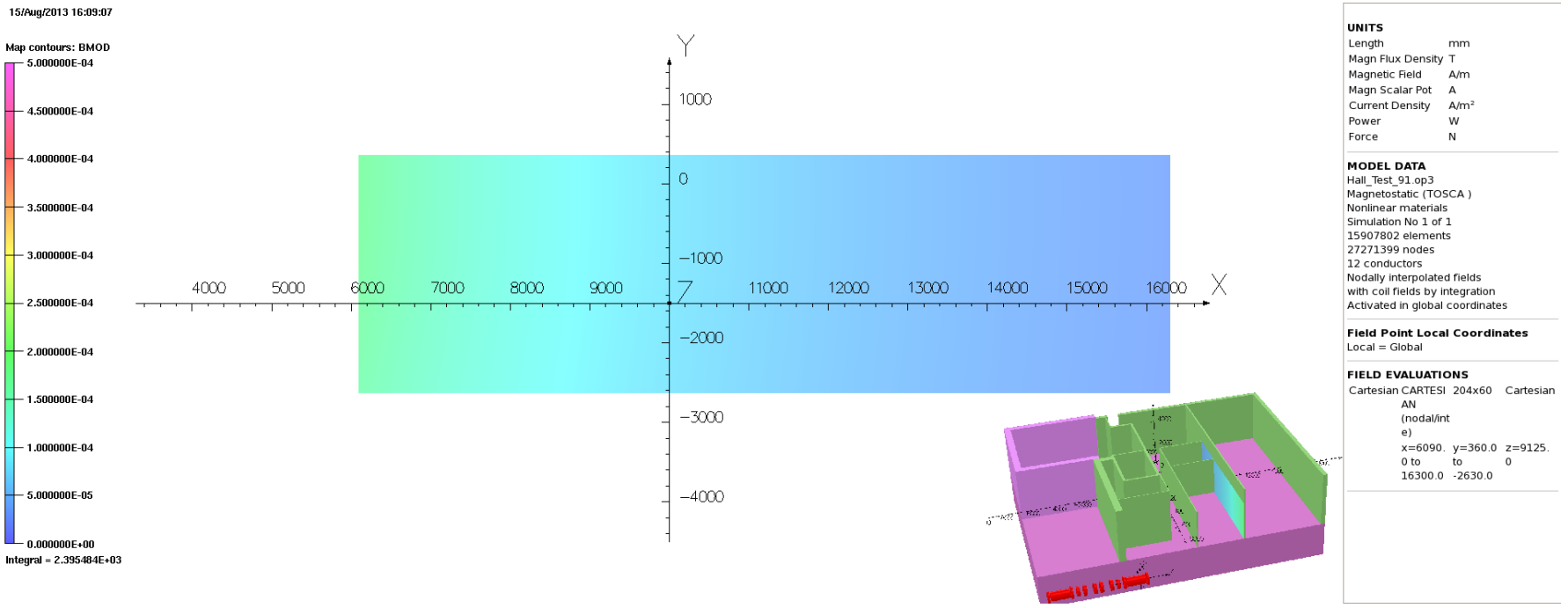

Figure 28: Bmod. Step IV 240 MeV/c Solenoid Mode. MLCR West Side.

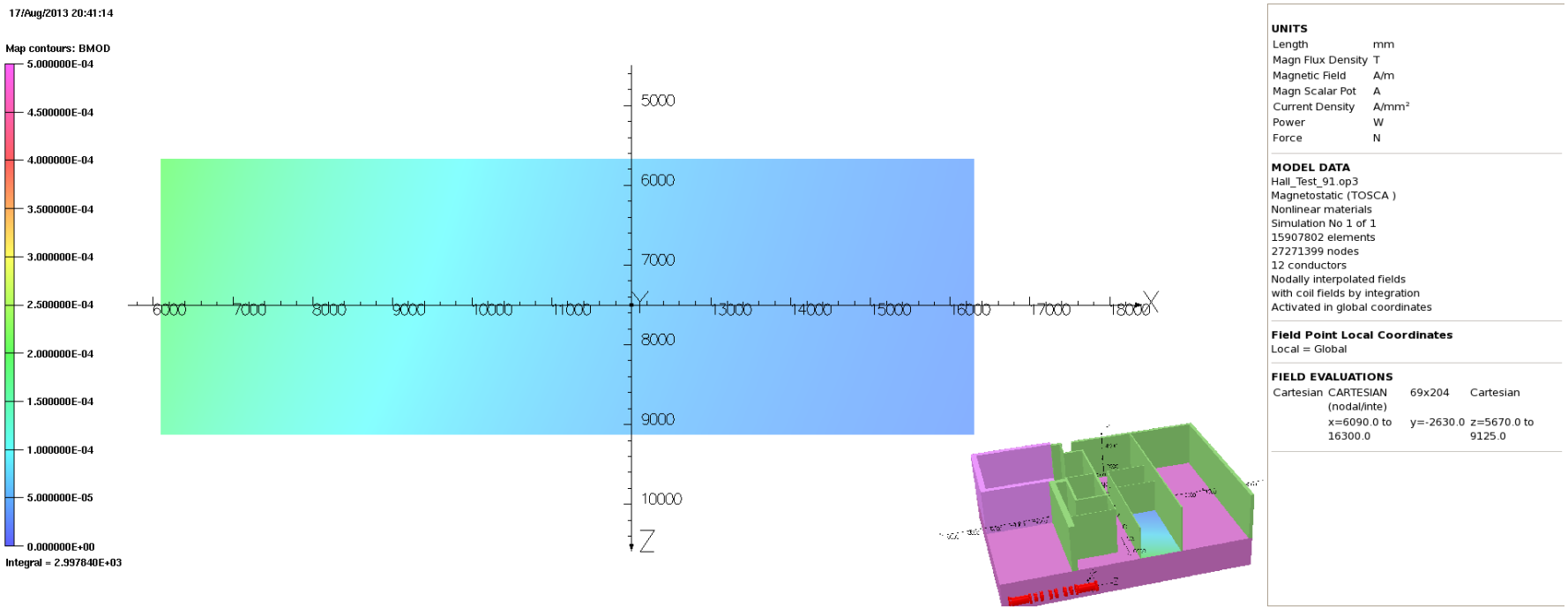

Figure 29: Bmod. Step IV 240 MeV/c Solenoid Mode. MLCR Floor.

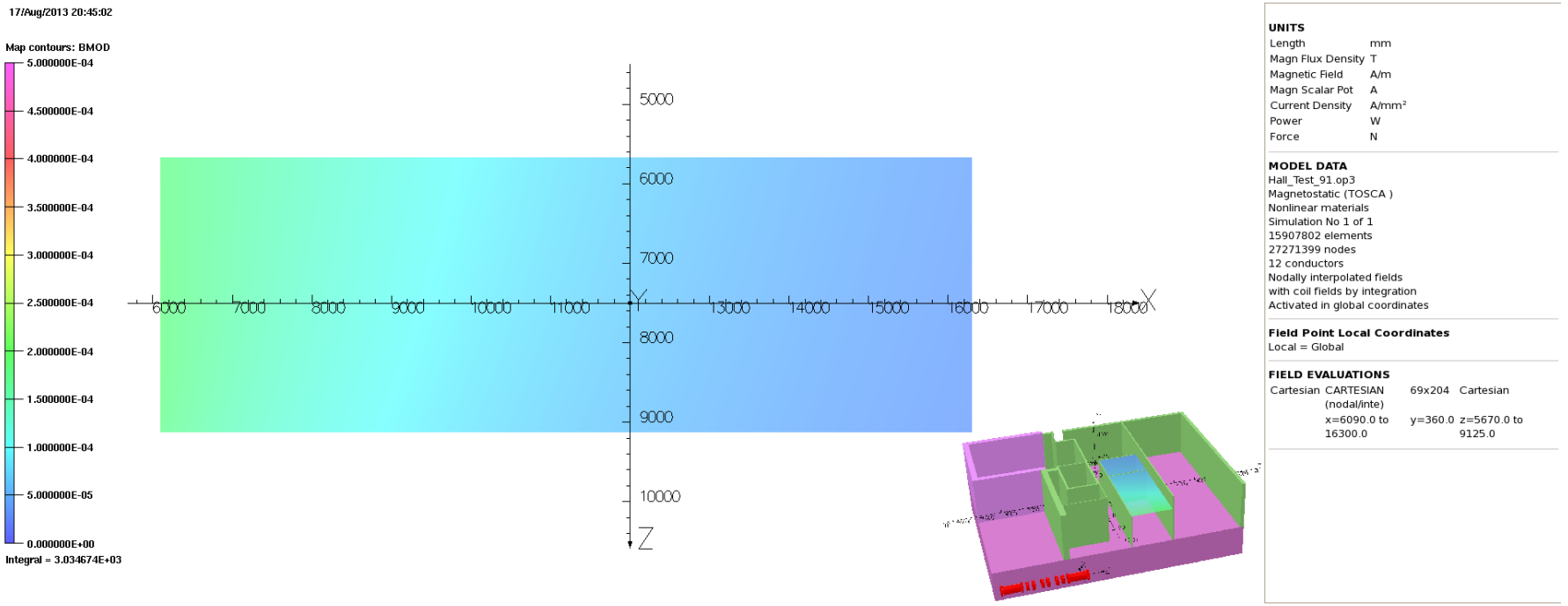

Figure 30: Bmod. Step IV 240 MeV/c Solenoid Mode. MLCR Ceiling.

3.1.6 Rack Room 2 (RR2)

Rack Room 2 is located in the South East Corner of the South Side Buildings and is indicated by the volume enclosed by magneta coloured wall in the ealier figure 23. The shape of the room as indicated in the model is only an approximation of its true shape, which is quite complex, however the volume shown by the FEA model encompasses the whole of RR2. The approximation was made to ease the modelling and the subsequent meshing, as the walls are non-magnetic and so are not a critical component of the simulation.

This room has been provided as overflow for MICE, and will be utilised to contain many of the racks that can no longer be placed in the MICE hall due to the stray field. Further details on this were presented in section [REFERENCE TO JASON'S SECTION]

RR2 is far enough away from the beamline that the additional fields imposed from Step IV running are negligible. Figure 31 shows a cross section of the field through this region at a height of y=-1000 mm below beam height level (All of the buildings on the south side of the MICE hall are slightly lower in elevation than the MICE hall itself.) and gives some indication of the predicted field strength in this region from the MICE magnets. The direction of the field can be seen in the earlier figure 24. As the predicted field strength is of the order of $\approx\leq 0.5$ gauss there are therefore no concerns with putting equipment into this room for MICE for Step IV.

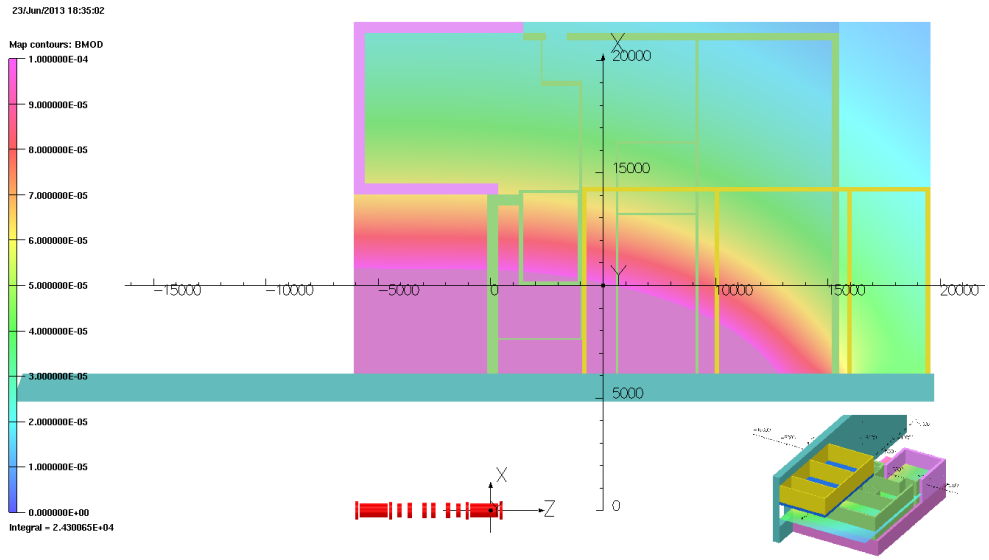

Figure 31: Bmod at y=-1000 mm. The fields through RR2 are negligble for Step IV. Note the scale on this plot is 1 gauss.

3.1.7 Behind the North Shield Wall (NSW)

The North Shield Wall is of interest because there are a number of electrical systems that sit behind this wall. Beyond Step IV the RF tubes, amplifiers and their associated electronics will be placed here. The North shield wall also partially shields the sub-station transformer, although this will be dealt with seperately in section 3.2.3.

The MICE fibre trackers sit inside the bore of the largest superconducting magnets; however the associated DAQ electronics are constrained to be within 10 m of the tracker due to the length of the leads. The length of these leads means that it is possible to place the tracker racks behind the North Shield Wall. ***LINK TO CRAIG'S PHOTO*** This will only work if several other key components of the tracker system can be successfully shielded against the magnetic fields from MICE which are particularly large in this area due to their proximity to the magnets. The section [*** INSERT LINK TO KIRIL'S WORK ***] shows the work done to understand the local sheilding requirements that would be necessary if global sheilding was not to be employed.

*** CRAIG CAN WE HAVE A COPY OF A DRAWING THAT SHOWS WHERE THE RACKS COULD BE PLACED? (and can this be included here?)***

Before showing these plots it is once again worth pointing out that the MICE hall model assumes that the shield walls are dual skinned contiguous sheets of magnetic AISI 1010 steel. In reality these walls are not contiguous but are constructed from plates built onto an I-beam frame and unfortunately there are signficant gaps between where these plates join onto the beams. These gaps lead to flux leakage, which means that the performance of the shield wall may be worse than that indicated in these models. This issue is looked at in more detail in section 3.2.2. It is worth commenting that without the advantage of any measurements to compare with these models, the magnitude of this effect remains an uncertainty.

Figures 32 and 33 give some indication of the expected field strength behind the NSW. Note that both of these plots are on a 10 gauss scale.

*** CRAIG IS THERE A CONCLUSION THAT WE WISH TO DRAW FROM THESE PLOTS? FEEL FREE TO INSERT YOUR OPINION ***

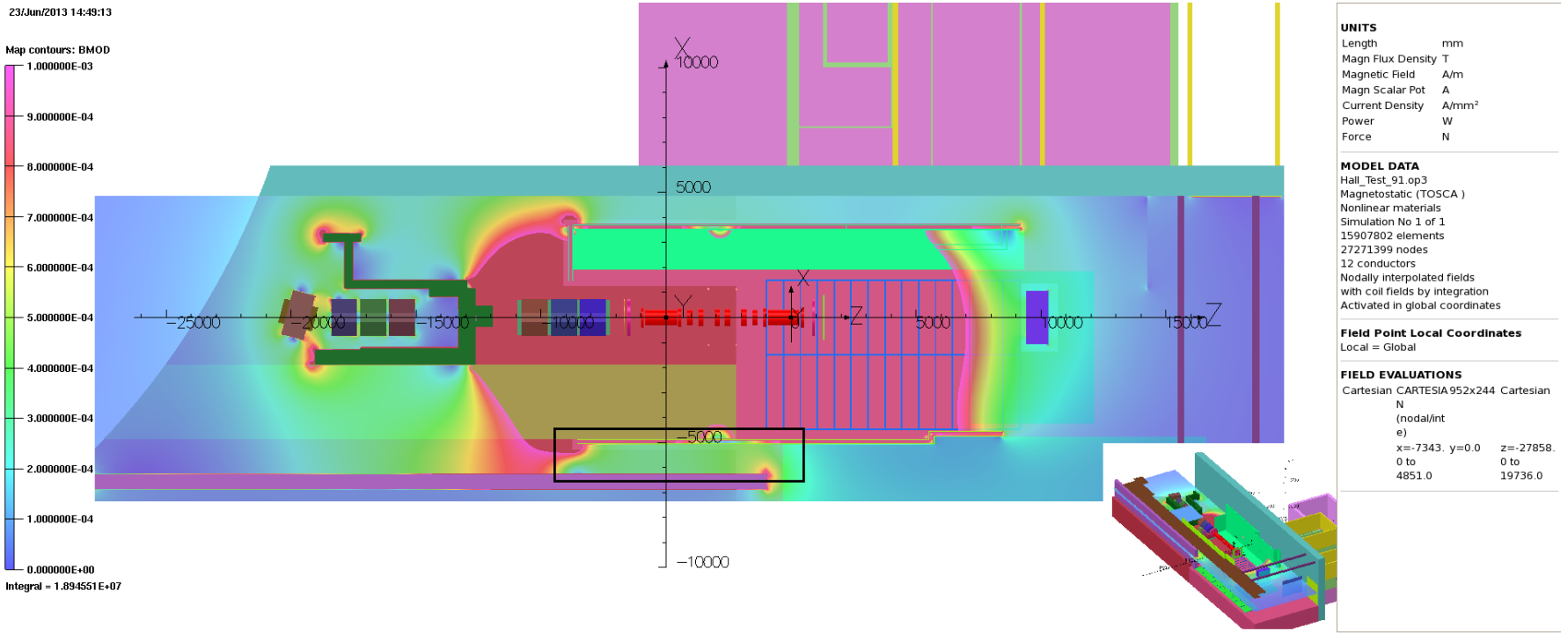

Figure 32: Bmod. Step IV 240 MeV/c Solenoid Mode. 10 gauss Scale. This is a plot at beam height. The area behind the NSW that sits between the Linac wall, marked with a black box, is noticeably warmer than the area behind the west end of the NSW.

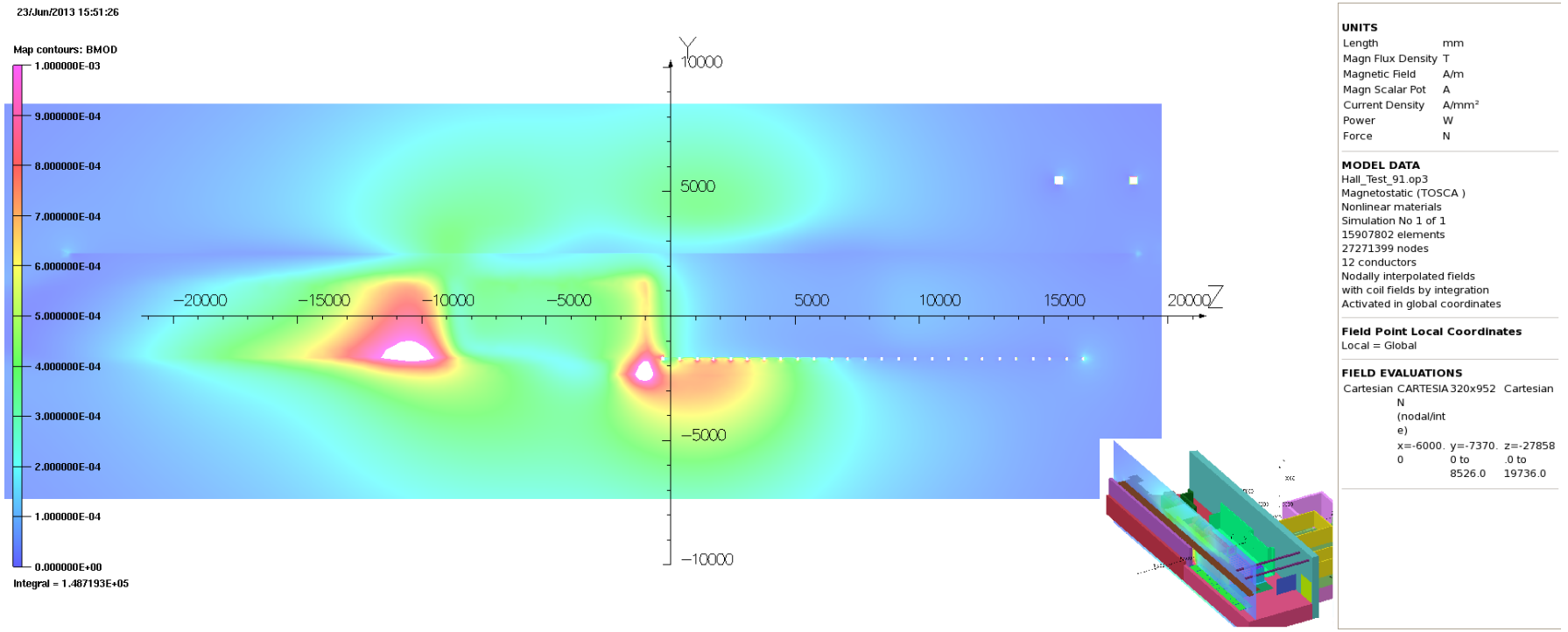

Figure 33: Bmod. Step IV 240 MeV/c Solenoid Mode. 10 gauss Scale. This is a plot at x=-6000 mm. See figure 32 to reference the plane. Once again it is clear that the area between the Linac wall and the NSW is seeing higher fields than behind the rest of the NSW

3.1.8 Quads Q7-Q9

Without the addition of a return yoke the Quads Q7-Q9 will see a significant magnetic field. In the hall model the quads have been modelled as a solid lump of iron, which clearly is an inaccurate overassumption, but on the scale of the hall model this simplification was necessary.

Figures 34 through to 35 show the effect that the quads are having on the field produced by the MICE magnets. There are a few points worth noting.

Firstly the downstream face of Q9 sees signficant magnetisation, however without a more realistic representation of the ferrous mass of a quad it is difficult to know whether this is a signficant real issue or not.

Secondly in the hall model the line of quads act as a low reluctance path to the flux providing a path to the DSA and the fridge plates on the South Shield Wall. This path to the fridge is unintended and has the effect of shifting the field further upstream. Once again the sensitivity of this to a real quadrupole ferrous mass is unknown.

In conclusion if a return yoke was not to be employed this is an area that would require further refinement and study.

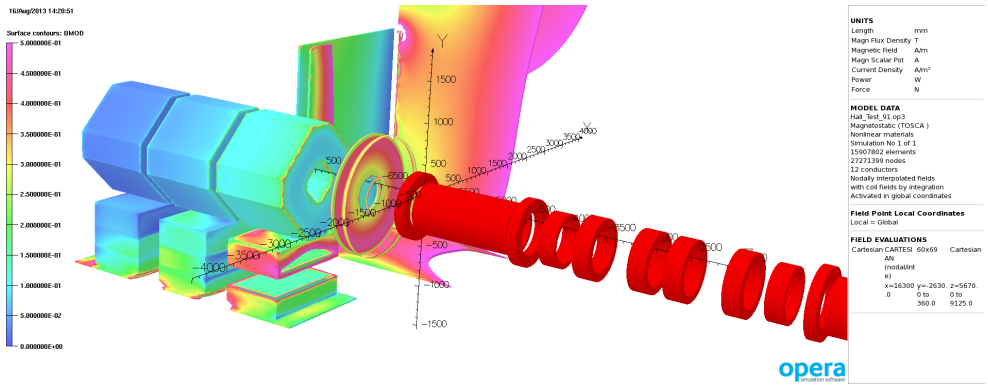

Figure 34: Bmod. 0.5T scale. Step IV 240 Mev/c Solenoid Mode. This shows the induced magnetisation in the ferrous components close to the magnets. The Quads, Q7 to Q9 left to right, have each been modelled as a solid ferrous lump, so the amount of iron has been overestimated. It is unclear what effect a more realistic model would have but it is clear that Q9 will see a large field from the cooling channel.

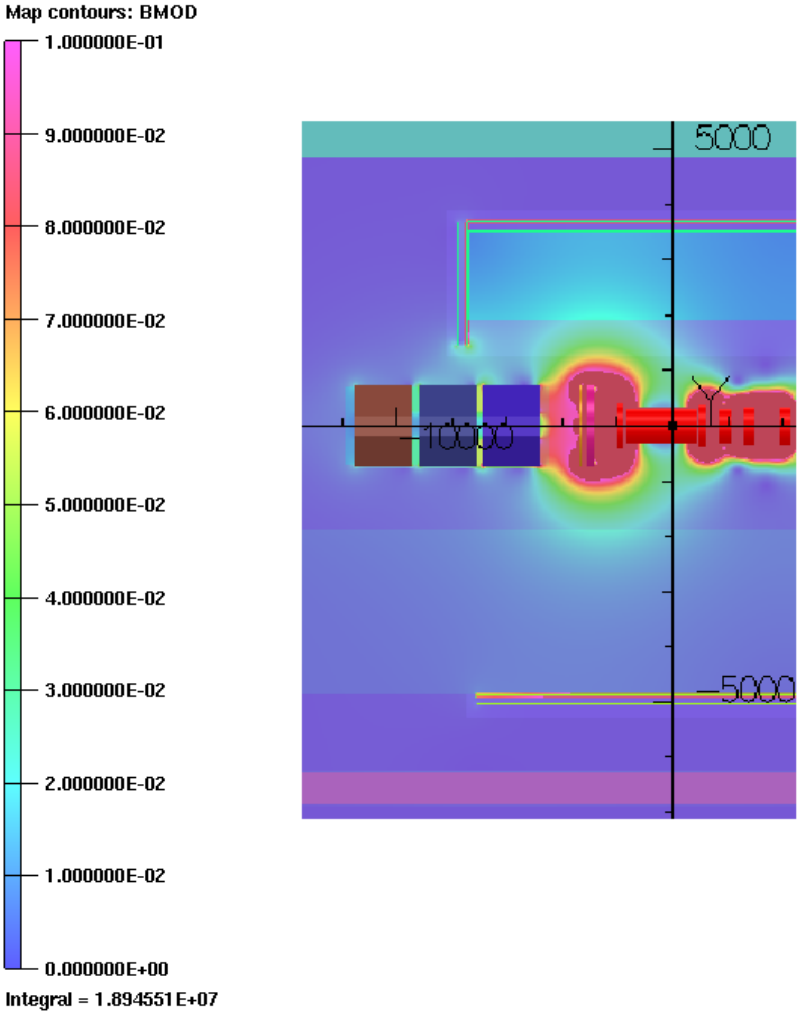

Figure 35: Bmod. 100mT Scale. Step IV 240 Mev/c Solenoid Mode . This plot shows how the quads pull the field from the magnets and how there is a hot spot around the end of the fridge plates; these are the plates that are part of the SSW and are perpendicular to the second quad, Q8, in the figure.

3.2 Sub Models

In order to study some features in further details, some sub-models were built. This section details these submodels and the results obtained from them.

3.2.1 Trench

*** I have added this subsection as I think Mike Courthold may have done some work on this and might wish to add something. If not then remove. *** Note I haven't yet asked him about this!

3.2.2 Shield Wall Model

Both the north and south shield wall are constructed from plates of AISI 1010 steel bolted onto a steel frame, however in the MICE hall model the shield wall is modelled as a contiguous sheet of AISI 1010 steel with no supporting framework.

In principle this should be a reasonable approximation, however it has been noted that the plates from which the real steel wall are constructed have significant gaps between the plates. Given that the structural steel behind the plates (I beams) has poorer magnetic properties than the face plates and that additionally the I beam it is much thinner in cross section there was some concern that the real wall will not perform quite as well as the modelled one. Will there be significant field leakage behind these gaps thereby increasing the effective field behind the shield wall?

In order to understand this issue a separate high resolution model of the shield wall was built incorporating these gaps to see if this effect was significant. The vertical I beams were included in the model, however the horizontal I beams were not included as this would have made the meshing difficult. As the return flux will be dominated by the plates in the horizontal direction the horizontal I beams are less important. The meshing of the model was very fine to capture the detail in the gap and to get an accurate representation of what is happening in the gap region. The model included the Step IV magnets at 240 MeV/c Solenoid mode.

The First section of wall that was modelled was composed of two by three panels. This model demonstrated that gap leakage would be observed but the model was of insufficient size to make suitable comparisons with the model of the shield walls in the MICE hall model. For brevity these results are not included here but are available online.

Subsequently a second model with a larger wall composed of three by seven panels was modelled. This wall is approximately half the size of one of the real shield walls. A 7 mm panel gap was used in all of the models. Figure 37 illustrates how the shield wall looks with respect to the Step IV magnets. The

Figure 36: Photograph of the north shield wall. The gaps between the plates can be clearly observed.

I beams can be seen jutting out from the between the two layers of plates. Figures 38 and 39 shows the magnitude of the field behind the 7×3 shield wall model at a distance of 25 mm and 250 mm respectively behind the shield wall. There are clear peaks behind the location of the I beams where the continuity of the plates are broken. In this particular model the plates are standing off from the I beams by 1.5 mm which is to simulate the fact that the join between the plates and the I beams is not too good. The 1.5 mm is excessive and so represents a worse case scenario but some of the two by three panel models had perfect contact between the plates and the I-beams and an increase in the magnitude of the field behind the shield wall was still predicted, although the magnitude of the effect was much subdued. The models are sensitive to the reluctance of this magnetic connection between the plates and the I-beams and it is difficult to estimate what the reluctance of this connection is. This remains a large uncertainty in the modelling.

Finally plots 40 and 41 shows a comparison with the predicted field behind the South shield wall in model 91. There is a small discrepancy in the location of these two shield walls (≈3%) but the difference in the predicted field due

to the gaps inbetween the plates is striking.

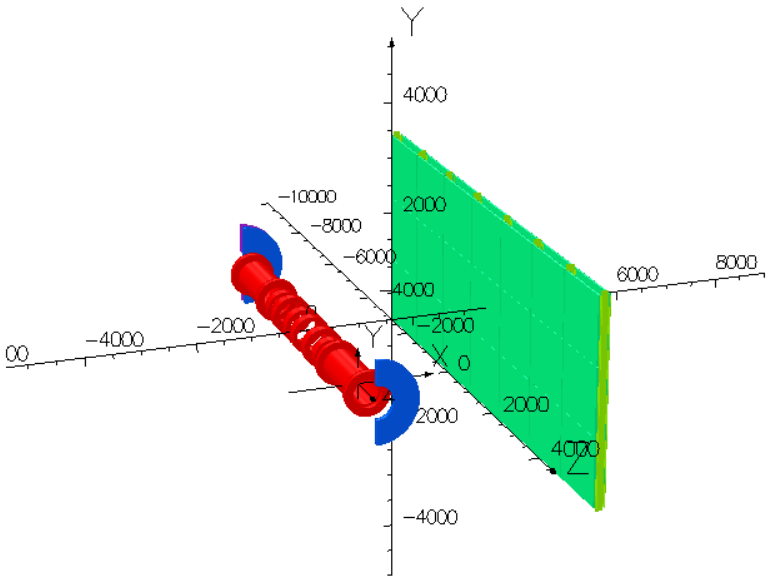

Figure 37: This shows the 7×3 shield wall model. The model is symmetrical in x and y to speed up the solve time. Consequently there is a symmetrical shield wall at the same distance on the -x axis that is not shown in this figure.

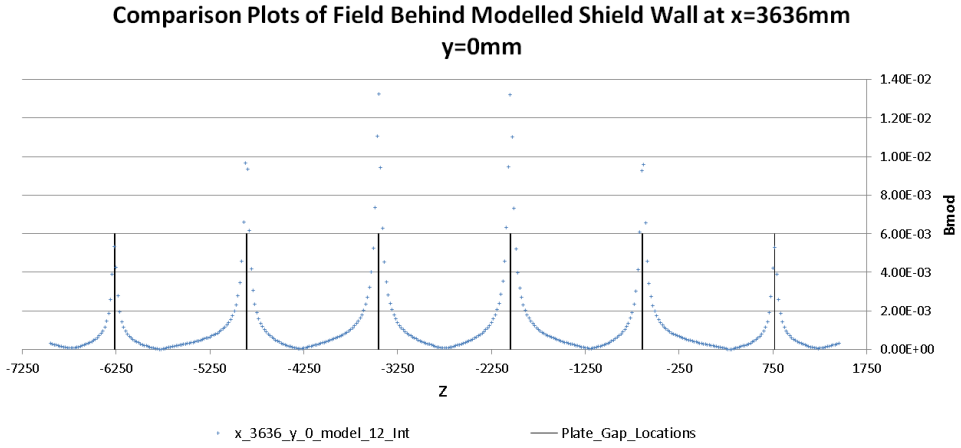

Figure 38: This shows the magnitude of the field behind the 7×3 shield wall model at a distance of 25 mm behind the shield wall. There is a 1.5 mm offset between the plates and the I-beams in this model

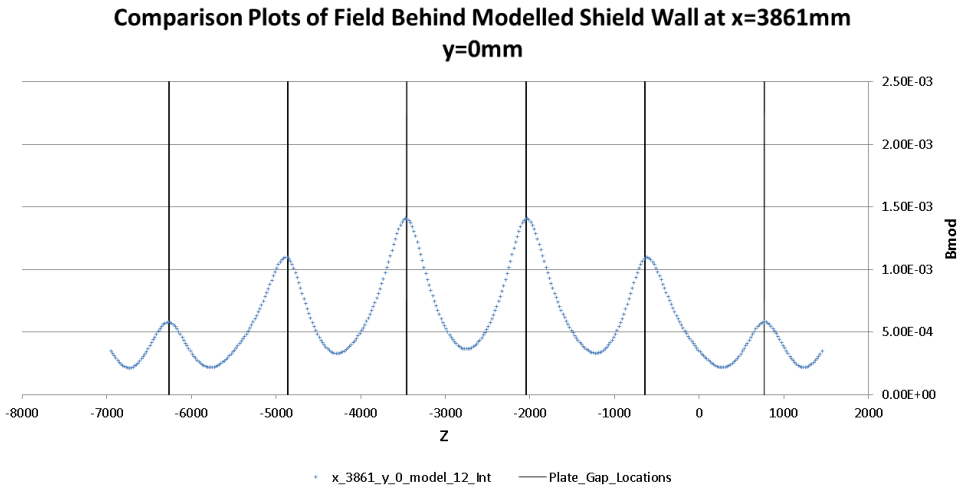

Figure 39: This shows the magnitude of the field behind the 7×3 shield wall model at a distance of 250 mm behind the shield wall. There is a 1.5 mm offset between the plates and the I-beams in this model

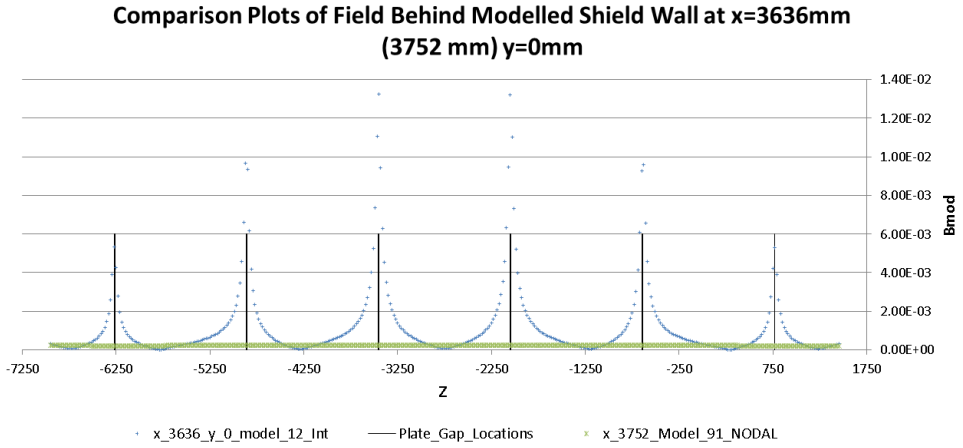

Figure 40: This is a comparison from plot (figure 38) compared with the predicted field 25 mm behind the South Shield Wall from model 91. The South shield wall is slightly further away from the magnets than the standalone shield wall model so the south shield wall data is taken slightly further away from the axis (3752 mm vs 3636 mm). Despite this small discrepancy in distance to the shield wall (≈3%) the difference in the predicted field behind the wall is striking.

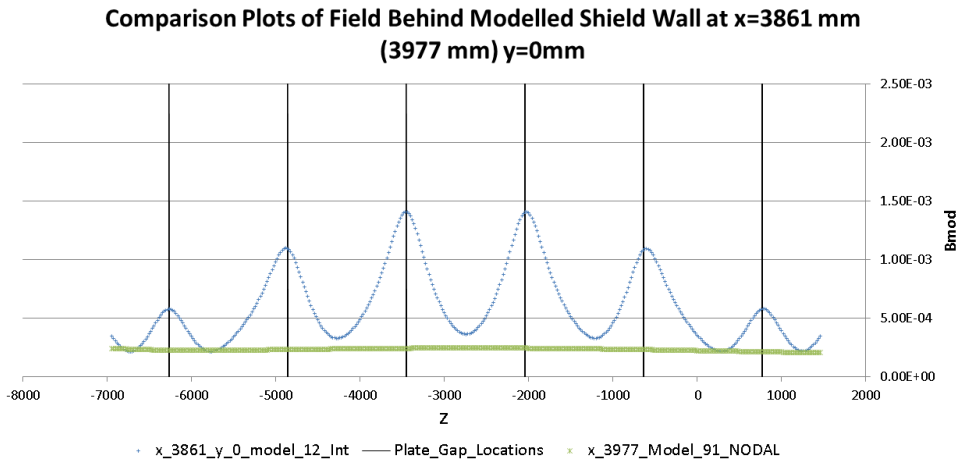

Figure 41: This is an identical comparison from plot (figure 39) compared with the predicted field 250 mm behind the South Shield Wall from model 91. As previously, the South shield wall is slightly further away from the magnets than the standalone shield wall model so the south shield wall data is taken slightly further away from the axis (3966 mm vs 3861 mm).

*** NOTE: I have included the results that we have but ideally I would like to re-run the shield wall model at the NSW distance with no gap, a 1 mm gap and no gap with a contiguous wall for comparison with model 91. As this is a computationally expensive model I will try to run this model over the summer holidays. If not then we will be stuck with what we have.

(It would also be nice to re-run these models at a distance that is comparable with SSW given that current model has a small offset error in it but this is less important.)

***

Conclusions

The shield wall models have indicated that for the case where the shield walls are not contiguous that any gaps in the shield wall do have an effect upon the field that is observed behind the shield wall. The increase and the localisation of this increase in the field are dependent upon a number of assumptions that are implicit within the model. It would be difficult to further quantify or justify these assumptions without recourse to some magnetic measurements. As we would be unable to obtain such measurement until the MICE magnets

are in-situ and turned on this leaves us in an uncomfortable situation that we have a known problem that is difficult to quantify.

This does leave several questions unanswered.

Is there a global increase in the field behind the shield wall due to the gaps (as the shield wall is less effective than anticipated) and how far does this extend?

How far do the local incursions extend?

Do these incursions affect any equipment? If we don't build a return yoke the is the shield wall considered to be a safe haven for the tracker racks?

Do these incursions affect any walkways that were assumed to be safe?

It was already anticipated that a return yoke would be needed for Step V/VI of the experiment so on this assumption any magnetic leaks from the shield wall are less likely to be of concern for the RF (which wouldn't be used until any return yoke was in-situ). However even with reduced external fields do these leaks create local non homogenous areas in the field that would have an adverse effect on the RF tubes? Would MICE be better off without the shield walls at all in this area? This is something that will need separate consideration once a decision has been made.

3.2.3 Sub-Station Sub Model

The MICE hall contains a modern substation that provides power for the experiment. This substation sits in the North West corner of the MICE hall and is partially shielded by the North Shield Wall. As the substation is relatively new there is a significant amount of control electronics, including programmable logic controllers, embedded into the substation's front panels. There is some concern that these electronics could be adversely affected by stray magnetic fields.

Figure 42 shows a photograph of the MICE substation. The base MICE hall model did not contain a model of the substation but the substation represents a signficant mass of iron, estimated at ≈5300 kg. In order to ascertain whether the substation would have an impact upon the field distribution in the MICE hall 5300 kg of mild steel in a 14 mm shell that was an approximate cuboidal representation of the substation geometry and location was added to model 91 and run as model 113. The results from this model through the plane y=0 can be seen in figure 46. Other figures can be viewed on-line.

Compared with model 91, there is minimal change to the field distribution in the area that the substation is located and it appears that the maximum air field that the substation will see is approximately 2 gauss, although for the most part the field is much lower. One can also ascertain that a significant field component runs South to North, although there is an East to West component at the West end of the substation. An equivalent model for Step VI of the experiment has not been run.

Figure 42: This photograph of part of the substation in the MICE hall clearly shows that a signficant amount of electronics has been mounted in the front panels.

To understand the effect of an external field on electronic equipment mounted on the surface of the substation panels several submodels were run where the substation was modelled as a series of racks with a 2 mm thick mild steel skin. The first set of submodels contained a single window in each rack that measured 450 mm high by 300 mm wide. The second set contained four windows in each rack, with each window measuring 100 mm by 100 mm on 150 mm width centres and 200 mm height centres. It should be noted that as only the outer panels were modelled these sub-models only give a total mass of 1000 kg but as we are primarily interested in the field level in the

windows of these 2 mm thick panels and that by and large the internal iron in these racks is some distance from these windows, this was considered to be sufficient to give a first estimate of the effect.

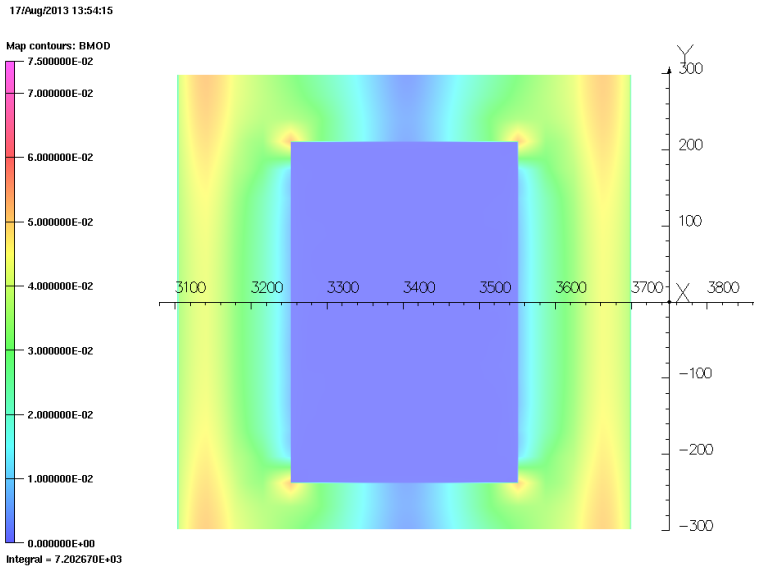

Figure 43: Plot of the steel around the second window from the West end in the substation model. 5 gauss external field running from South to North (from +x). 750 gauss scale.

An external field of 5 gauss was applied to these models, this was a deliberate overestimate of the external field based upon the air field results from model 91; some of the the submodels were completed before model 113 was solved. The submodels were run with both the field in a South to North direction and in and East to West direction for comparison. As none of the steel in the submodels is saturated then the results should to first order scale to a lower air field.

Figure 47 shows a cross section through the substation model at y=0 with a 5 gauss field from +x (South to North). This is a model with a single large window in each rack. One can immediately see that the area around the windows is seeing a field of approximately 5 gauss.

Figure 43 and 44 shows a couple of view of one of the windows in the submodel. The first image shows the steel surrounding the window and it's relative magnetisation. The other plot shows the predicted field strength in the window on a 10 gauss scale. One can see that the field in the window

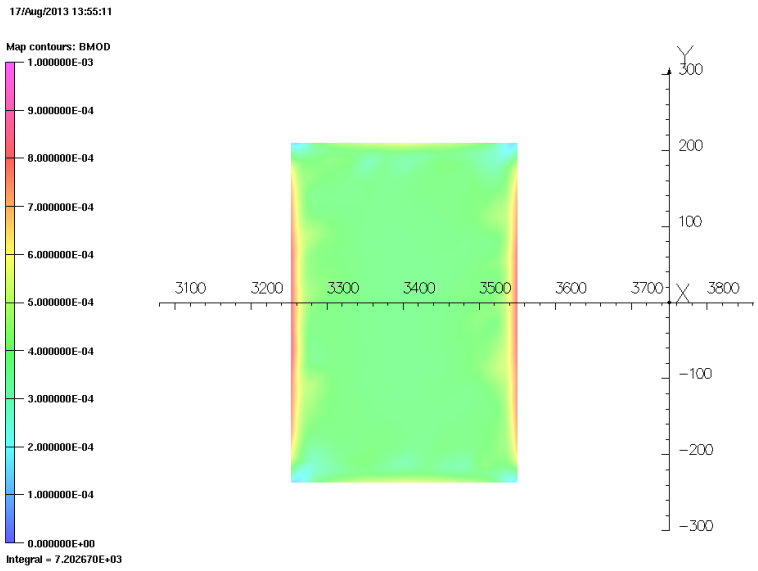

Figure 44: Plot of the air volume inside the second window from the West end in the substation model. 5 gauss external field running from South to North (from +x). 10 gauss scale.

is approximately the same as the applied external field (5 gauss) although there is some intrusion of higher field from the left and the right.

When the external field is applied East to West, a similar picture emerges except that the window plots see a slightly higher field of ≈20% and there is more intrusion of the field from the steel into the window space - see figure 45. A similar picture is seen for models that contain sets of four smaller windows instead of the one larger window.

Conclusions

The conclusion from these submodels is that for Step IV the substation does not appear to significantly alter the field profile and consequently the models predict that the substation will see a maximum field of approximately 2 gauss. Further submodelling indicates that any instrumenation mounted in the 2 mm thick steel panels will not see significant amplification of the external magnetic field due to their proximity to these steel panels and that the instruments should only see a level of magnetic field that is consistent with the magnitude of the external air field or slightly above it. A slightly higher level of magnetic field can be expected at the edges of the cutouts/windows.

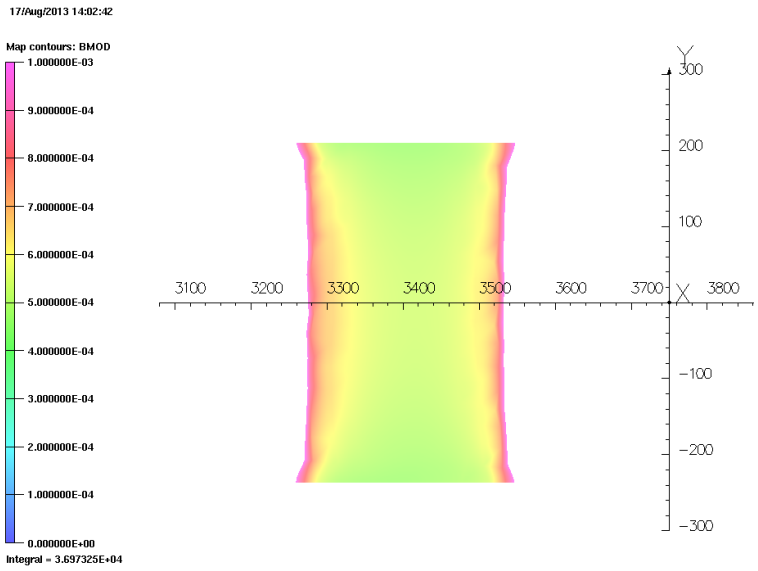

Figure 45: Plot of the air volume inside the second window from the West end in the substation model. 5 gauss external field running from East to West (from +z) 10 gauss scale.

It should be bourne in mind that these conclusions are based upon the predictions from the model only and these have no grounding in any field measurements. Consequently as the models are only an approximation to both the substation geometry and mass distribution the output from these models should be viewed as a guide.

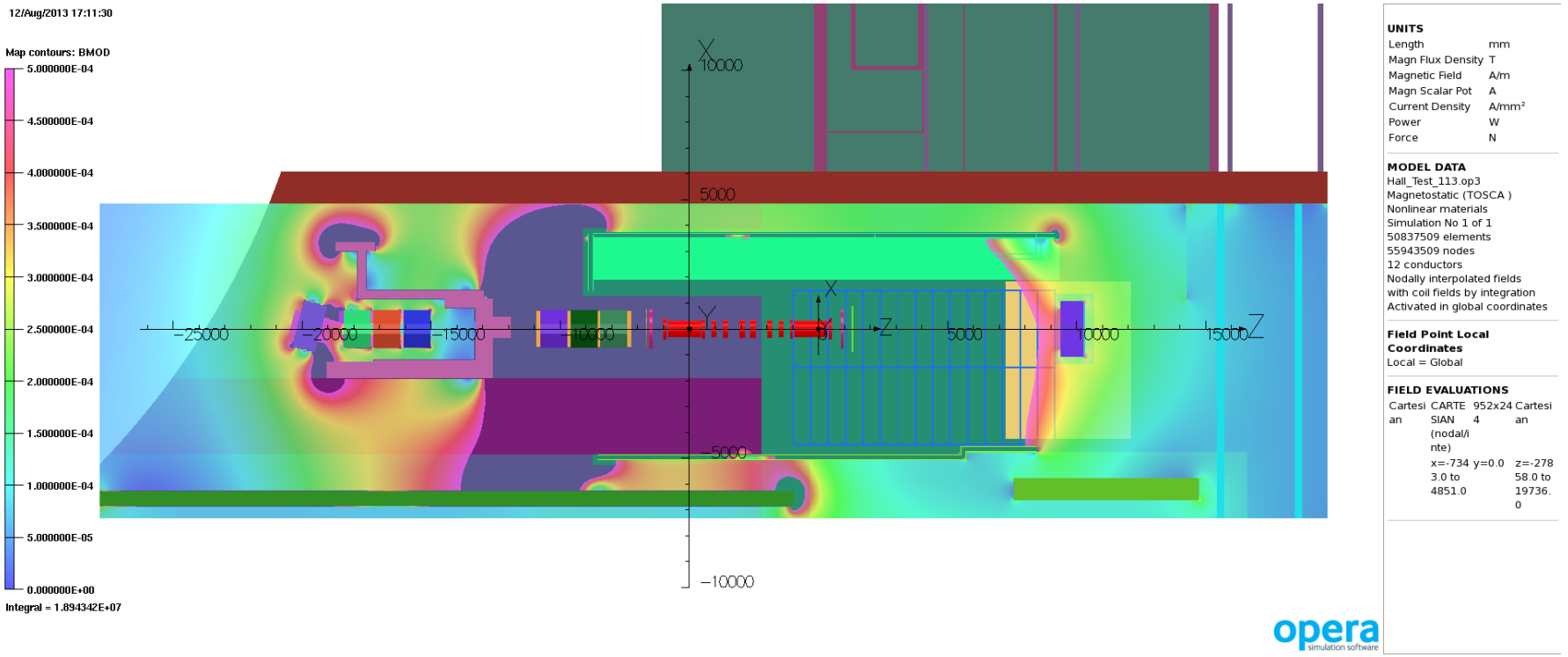

Figure 46: This is an image from the Hall model with the sub-station mass added - Model 113. Step IV Solenoid mode 240 Mev/c. The addition of the substation pulls the field slightly towards the north shield wall but change in the field distribution is minor.

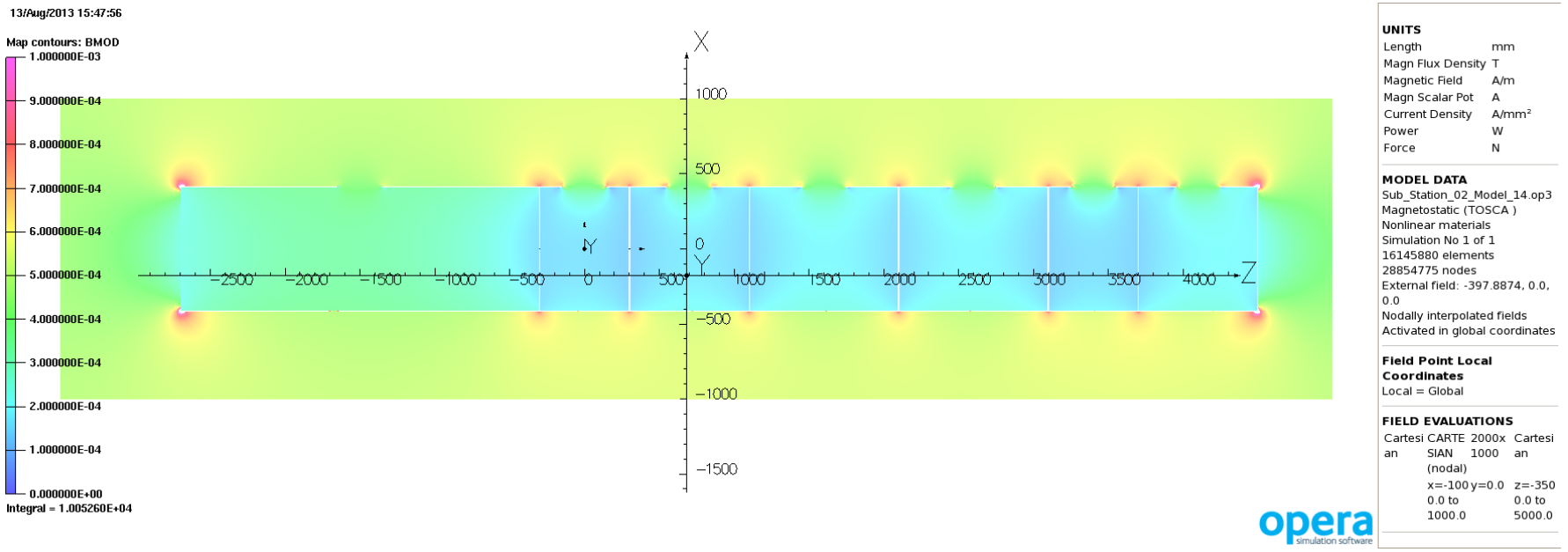

Figure 47: Bmod. Substation model. 5 gauss external field applied from +x (South to North). Note that the model boundary is much further out than the limits of the plot. 10 gauss scale. The field in the vicinity of the windows can be clearly seen.

Appendices

A Overview Plots for Step VI

This appendix shows the equivalent overview field figures for Step VI of the experiment and follows on from those plots shown in section 3.1.1. Like Step IV, solenoid mode appears to produce more stray field as there is some cancellation in flip mode.

Much less work has been done with the Step VI plots, as the focus has been primarily on Step IV, and there has been no comparative Biot-Savart calculations to compare the results of these Step VI simulations with. However these models are based upon the same model elements as the step IV model and so are provided as for comparison.

As with the Step IV plots all of these plots, and many more, are available online at the modelling website as high resolution images.

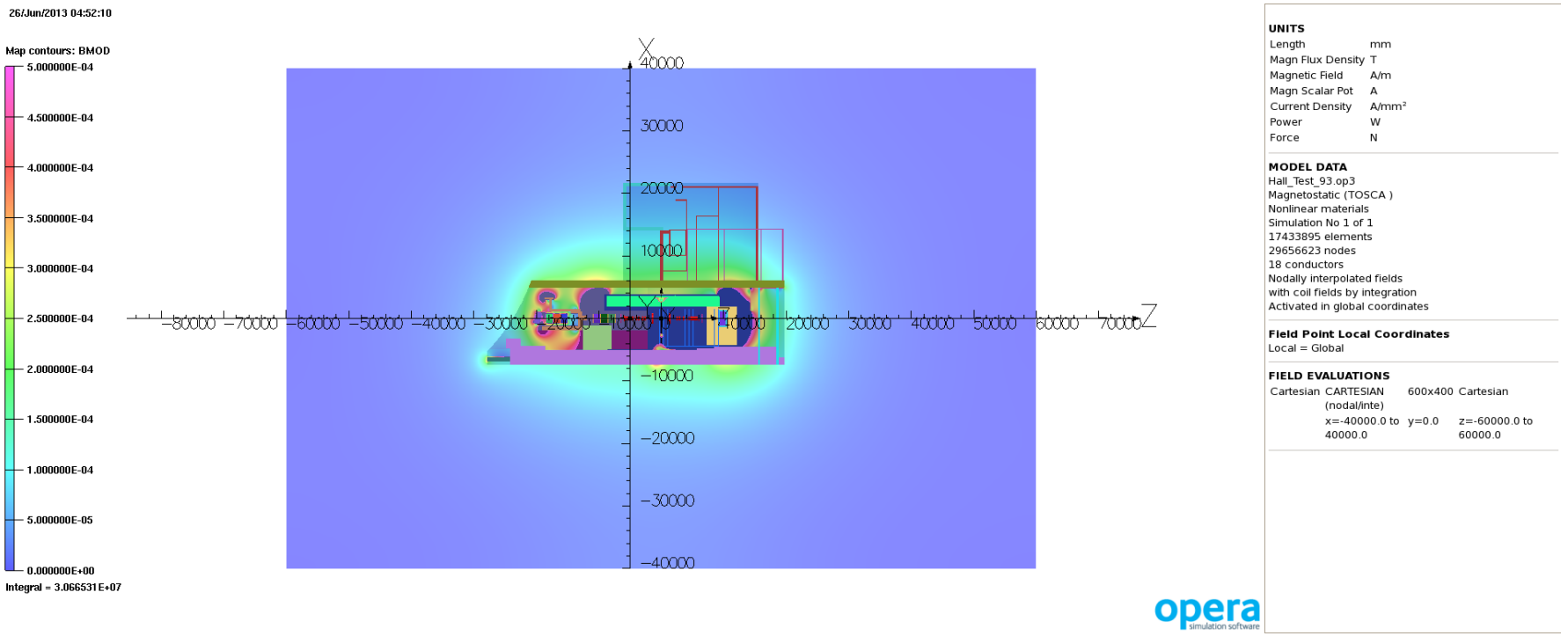

Figure 48: Bmod 5 gauss scale. Step VI 240 Mev/c Solenoid Mode. Overview of Model Volume at Beam Height from Model 93. The Model is shown with structures turned on. One can immediately see that the majority of the stray field is contained within the MICE hall.

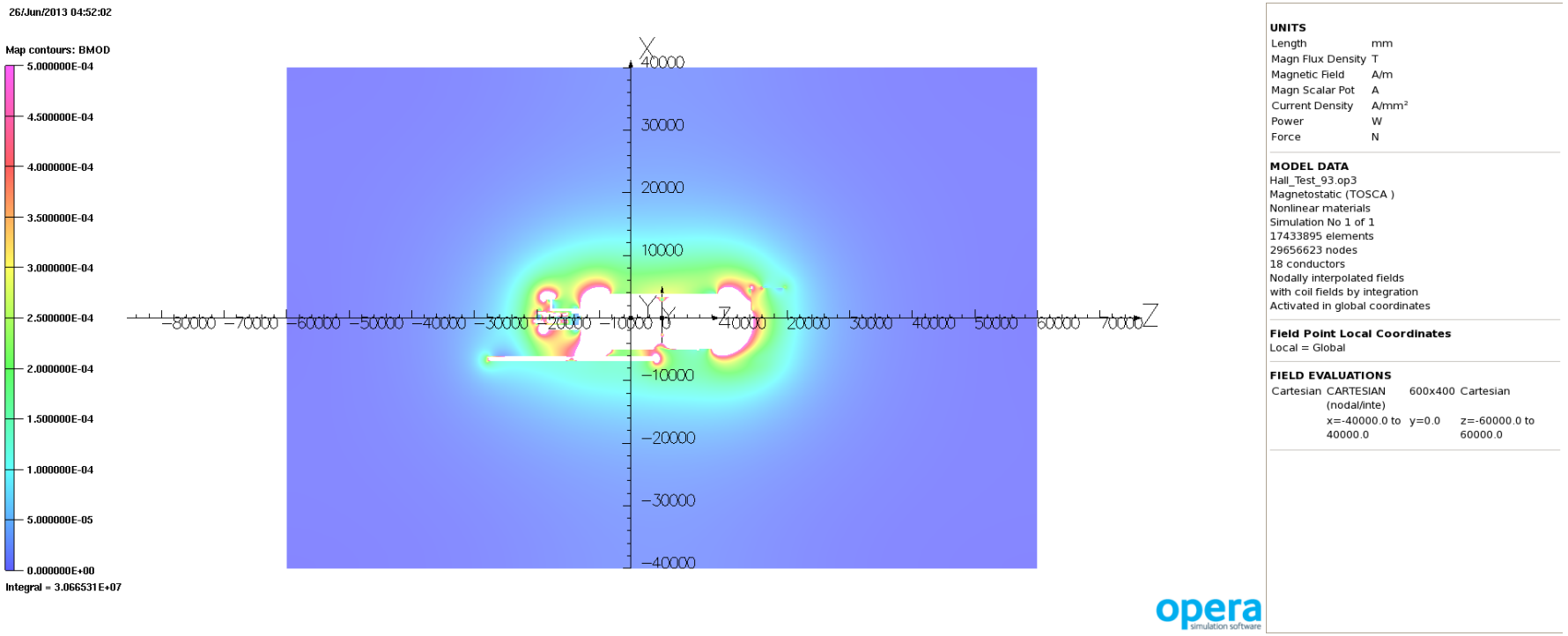

Figure 49: Bmod 5 gauss scale. Step VI 240 Mev/c Solenoid Mode. Overview of Model Volume at Beam Height from Model 93. The Model is shown with structures turned off.

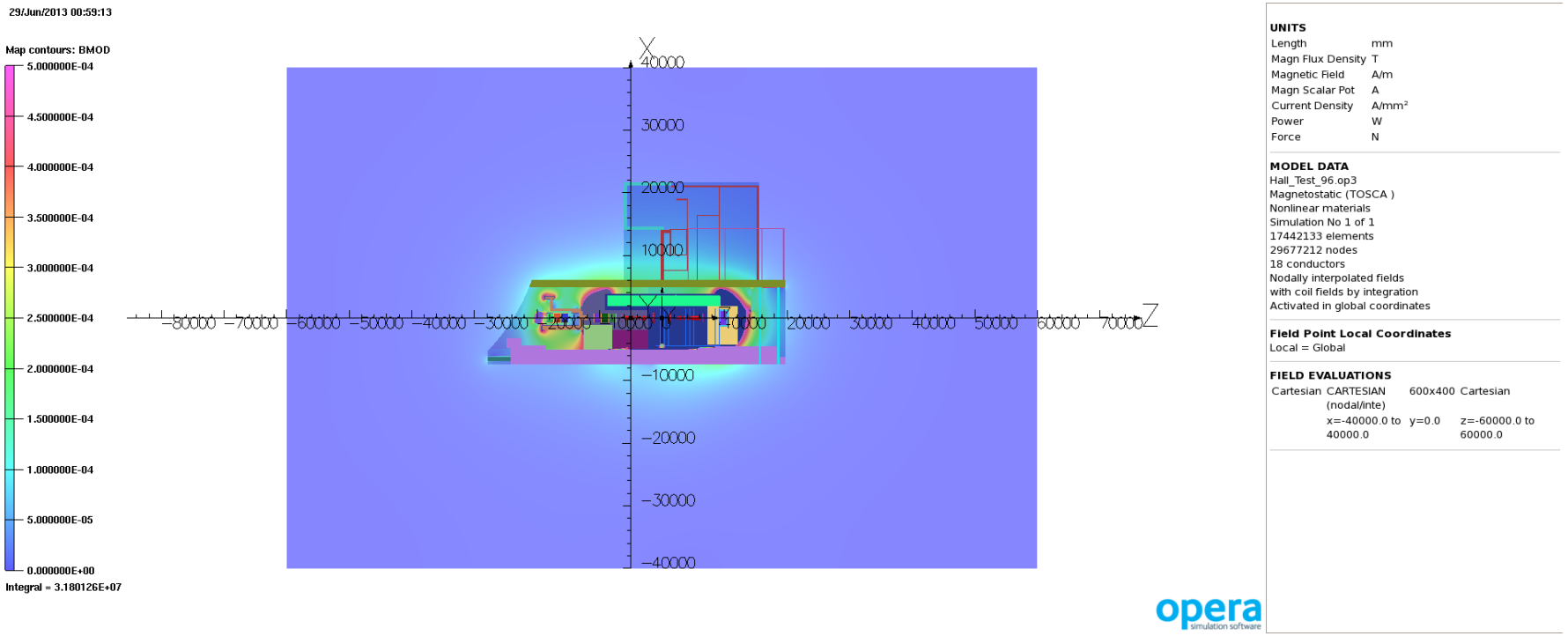

Figure 50: Bmod 5 gauss scale. Step VI 240 Mev/c Flip Mode. Overview of Model Volume at Beam Height from Model 96. The Model is shown with structures turned on. One can immediately see that the majority of the stray field is contained within the MICE hall.

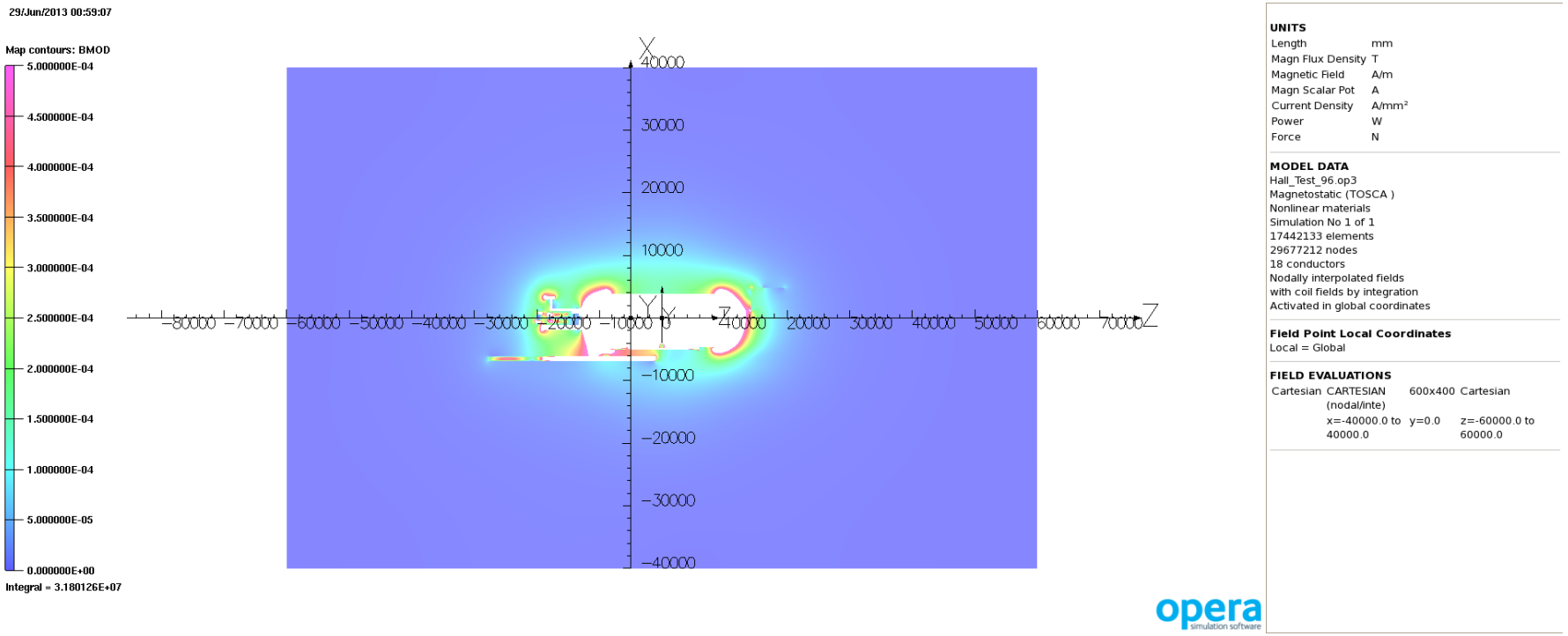

Figure 51: Bmod 5 gauss scale. Step VI 240 MeV/c Flip Mode. Overview of Model Volume at Beam Height from Model 96. The Model is shown with structures turned off.

B Fields on the outside wall of the MICE Hall - Step VI

This figures in this appendix show the field on the outside of the MICE hall for Step VI of the experiment and follows on from those plots shown in section 3.1.2.

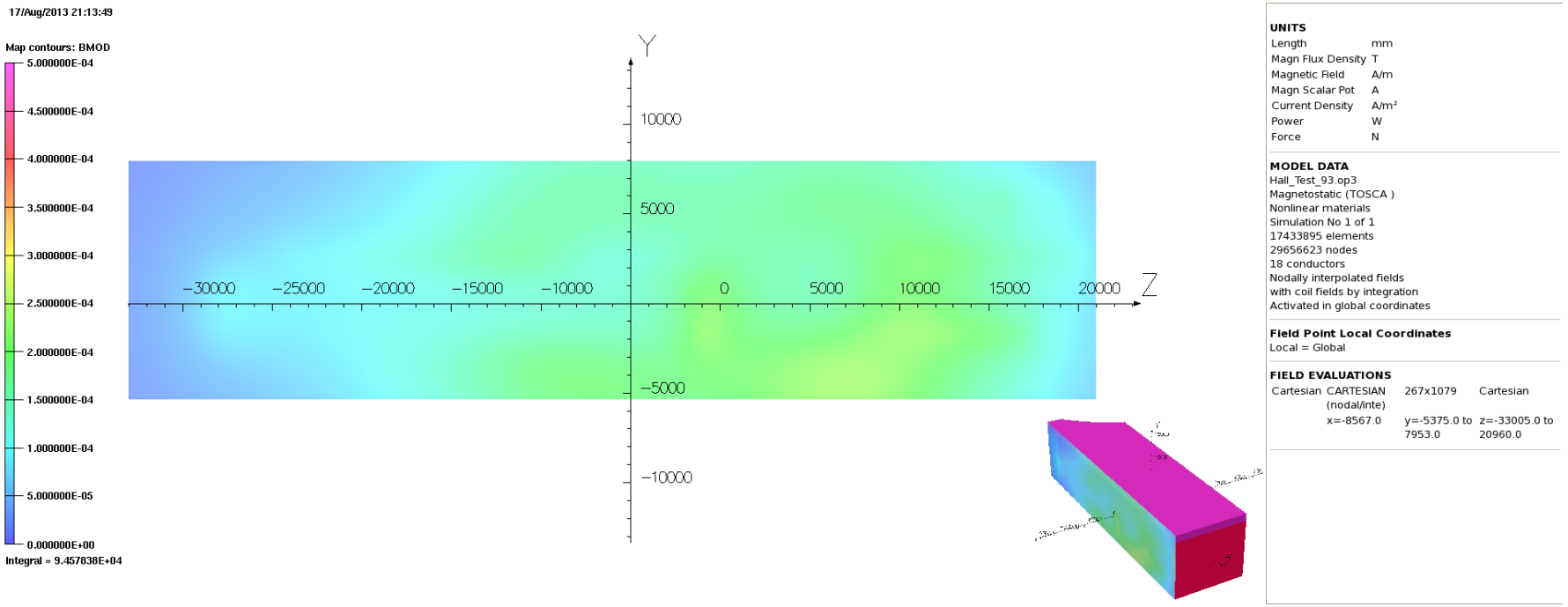

Figure 52: Bmod 5 gauss scale. Step VI 240 MeV/c Solenoid Mode. North Wall Side view.

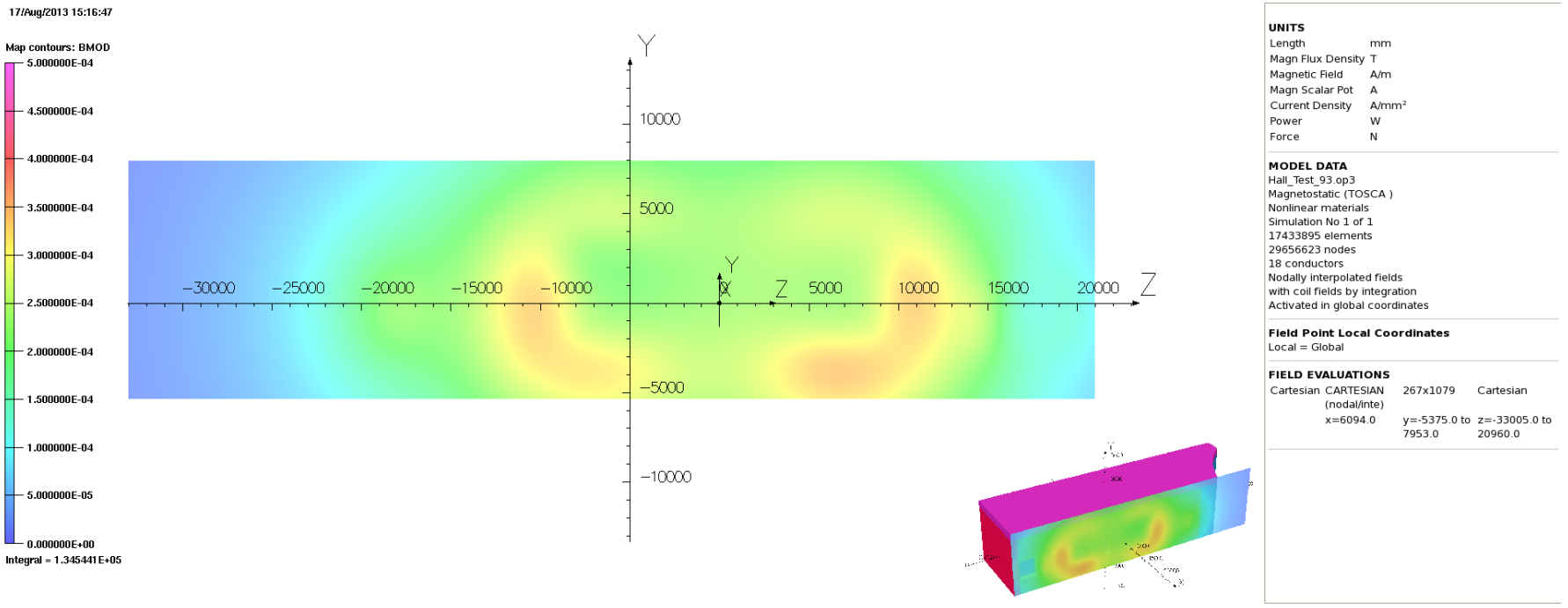

Figure 53: Bmod 5 gauss scale. Step VI 240 MeV/c Solenoid Mode. South Wall Side view.

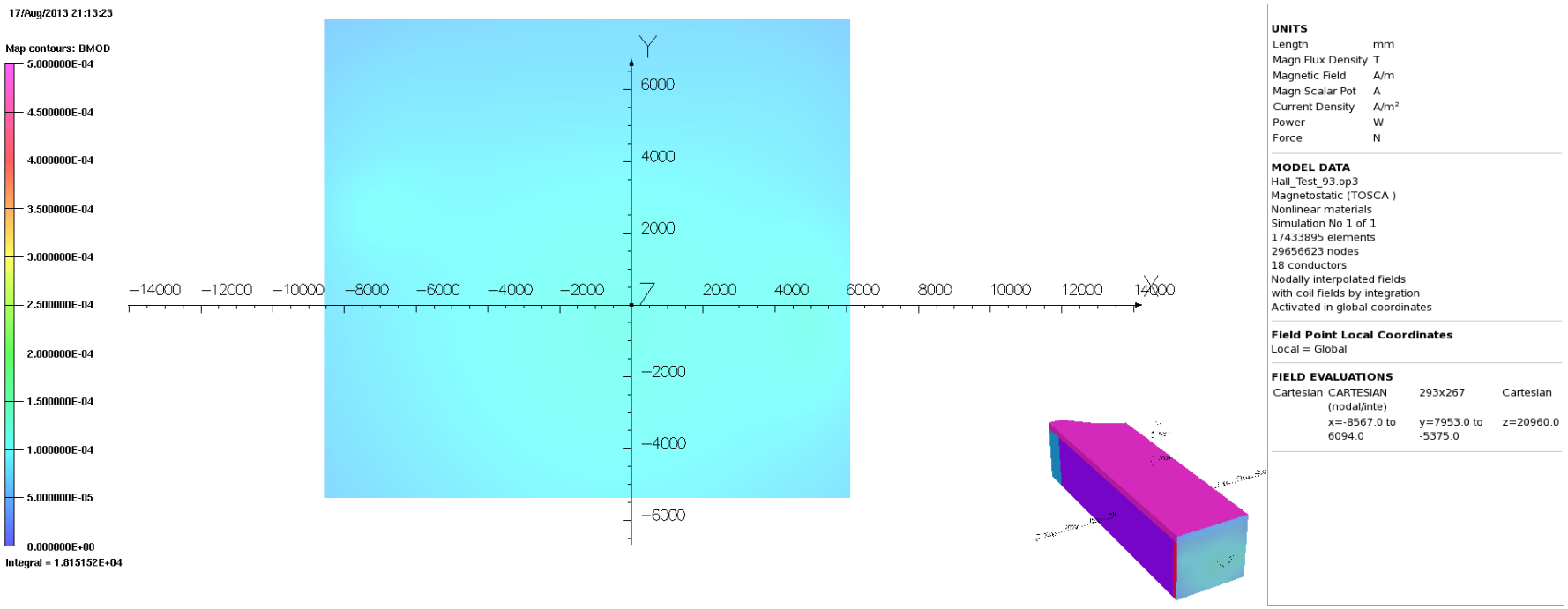

Figure 54: Bmod. Step VI 240 MeV/c Solenoid Mode. West Wall Isometric view. The predicted field is the same magnitude as that of the earth's magnetic field.

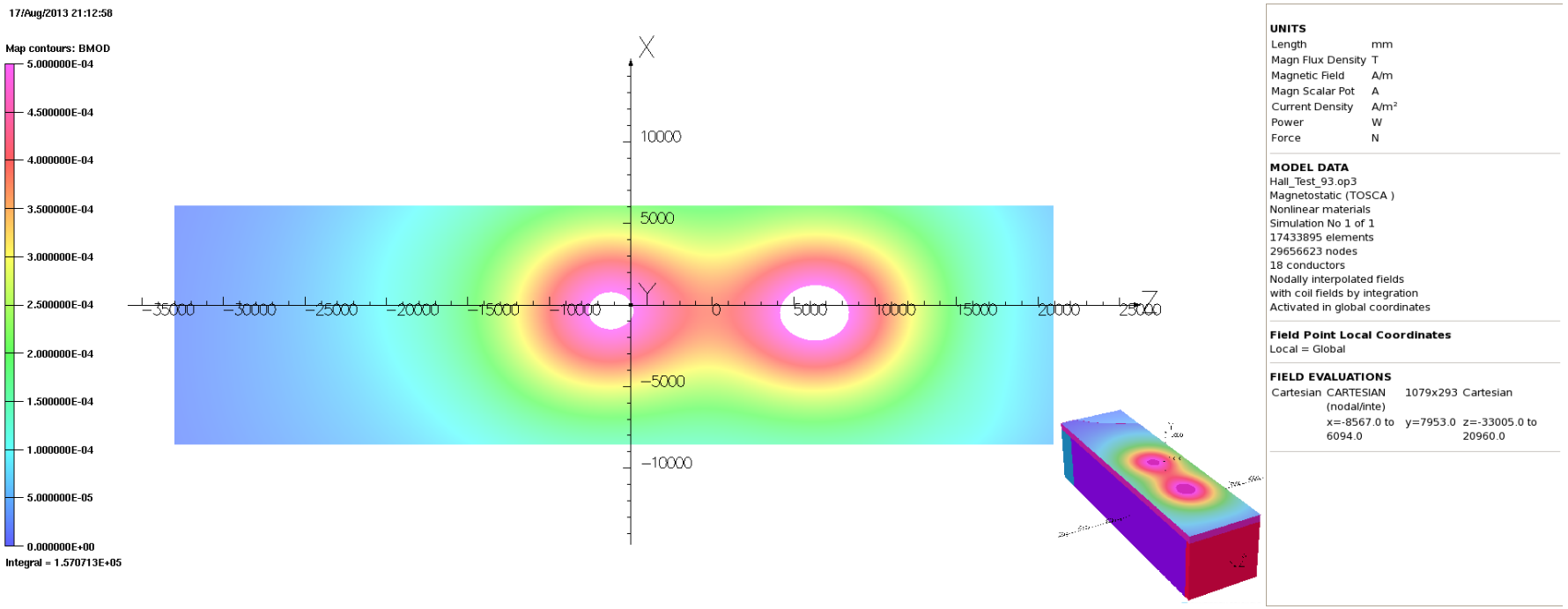

Figure 55: Bmod. Step VI 240 MeV/c Solenoid Mode. External to Roof. This is the only plot where the external field goes above 5 gauss.

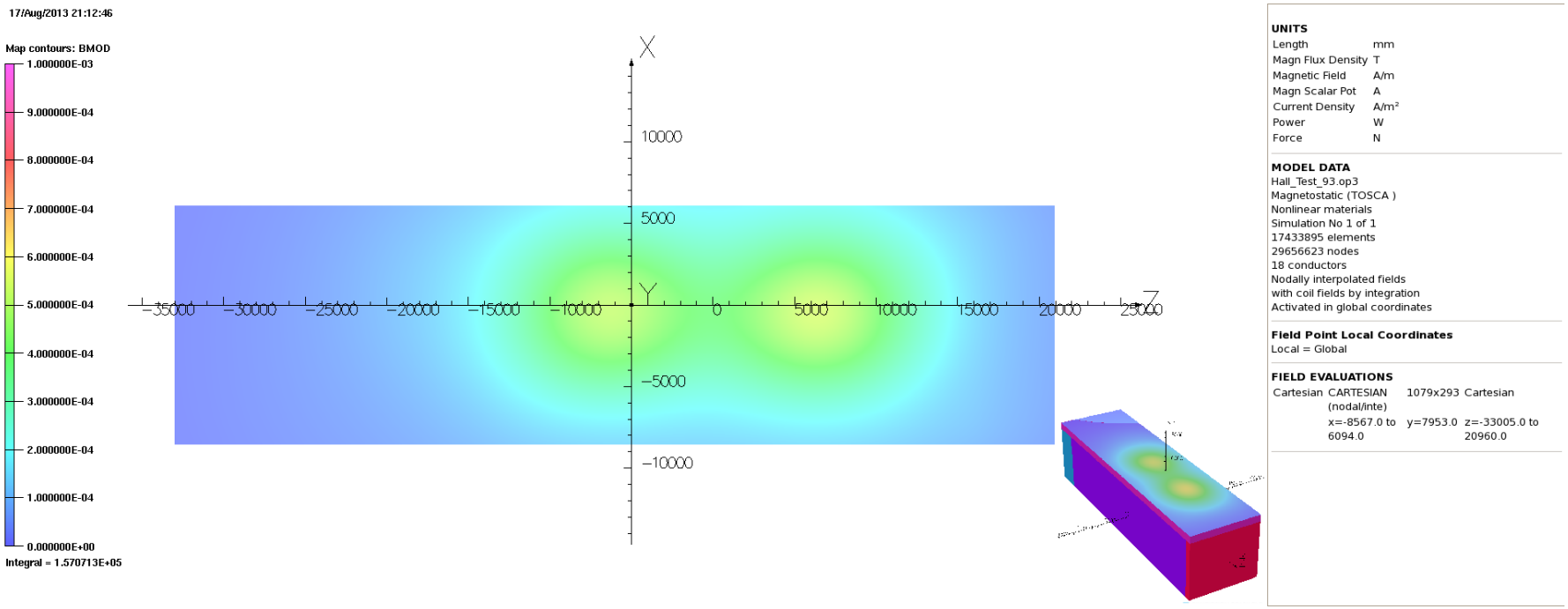

Figure 56: Bmod. Step VI 240 MeV/c Solenoid Mode. External to Roof. This is a 10 gauss plot of the roof. The peak areas are only just above 5 gauss.

C ISIS Control Rooms - Step VI

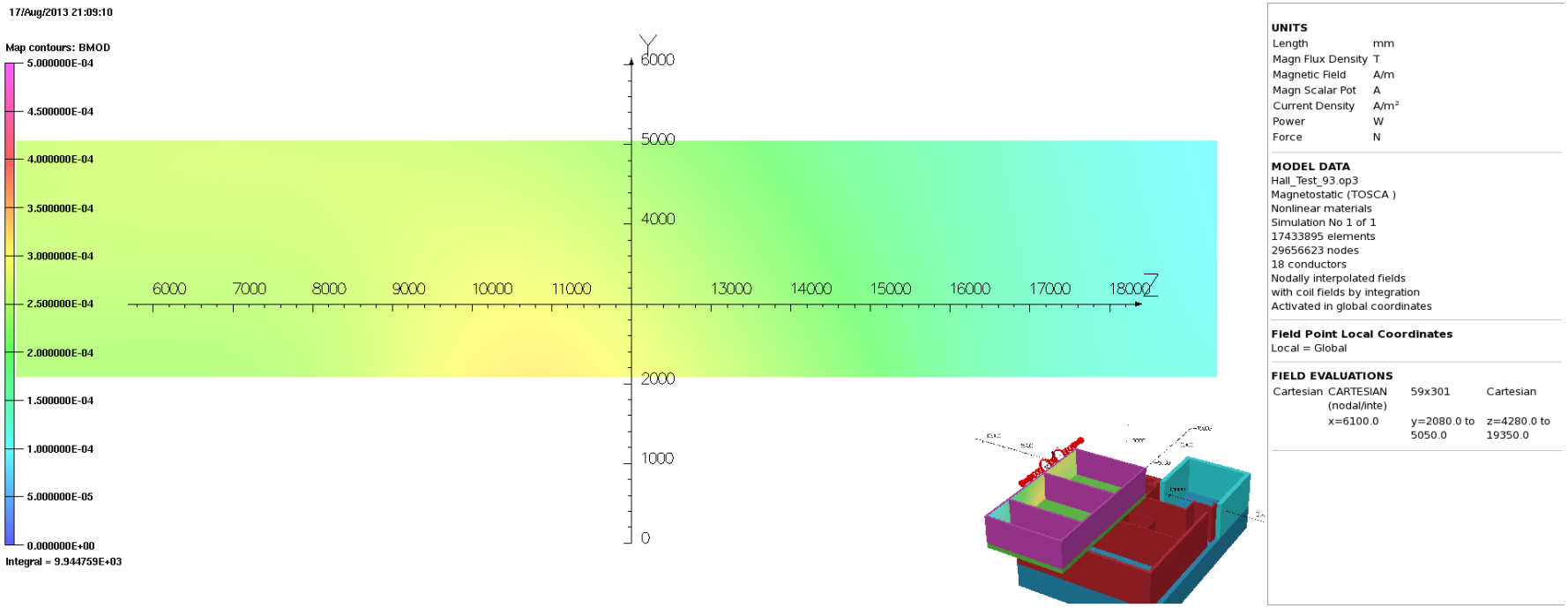

Figure 57: Bmod. Step VI 240 MeV/c Solenoid Mode. South Side of the ISIS control rooms.

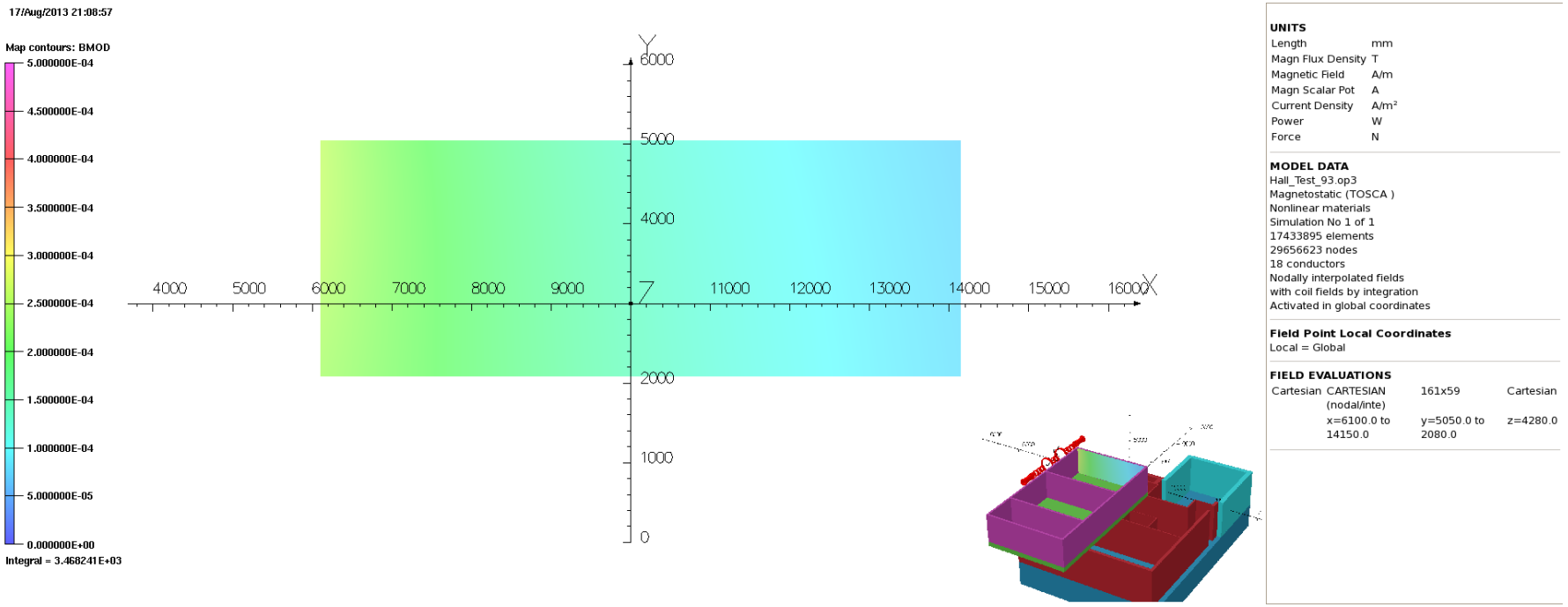

Figure 58: Bmod. Step VI 240 MeV/c Solenoid Mode. East side of the ISIS control rooms.

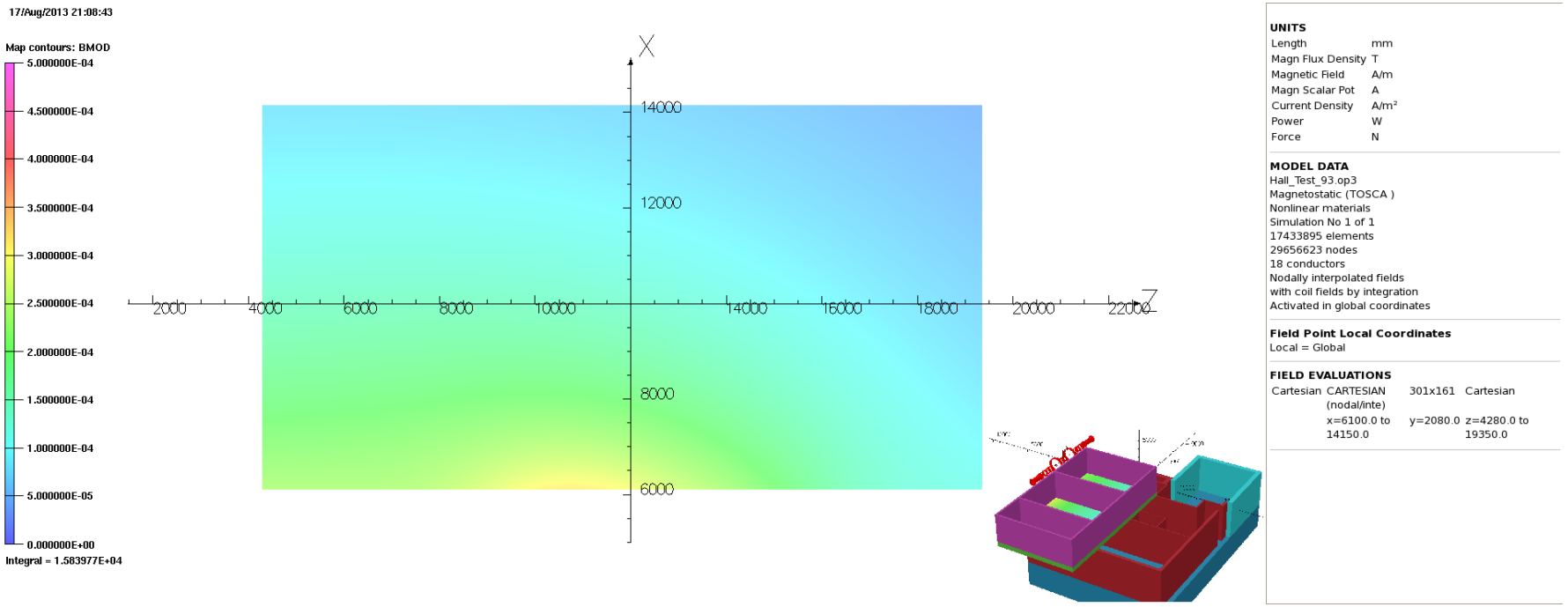

Figure 59: Bmod. Step VI 240 MeV/c Solenoid Mode. Floor of the the ISIS control rooms.

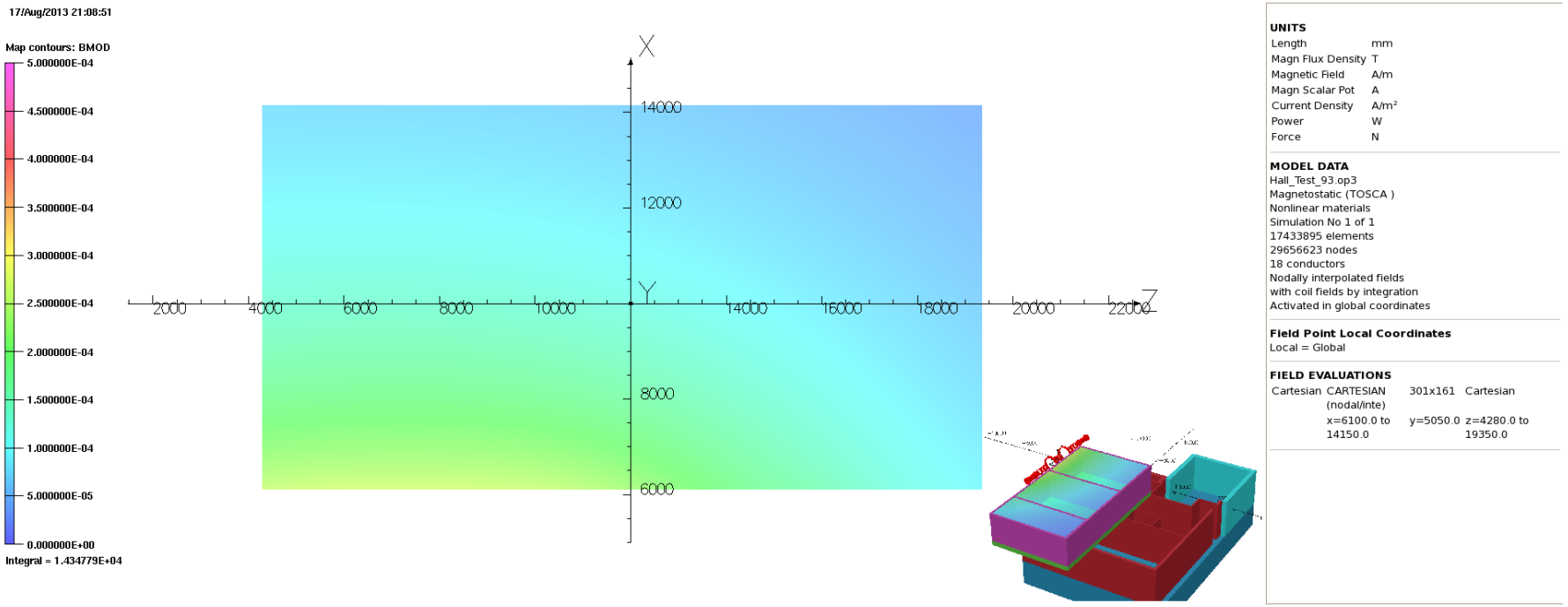

Figure 60: Bmod. Step VI 240 MeV/c Solenoid Mode. Ceiling of the the ISIS control rooms.

D MICE Local Control Room - Step VI

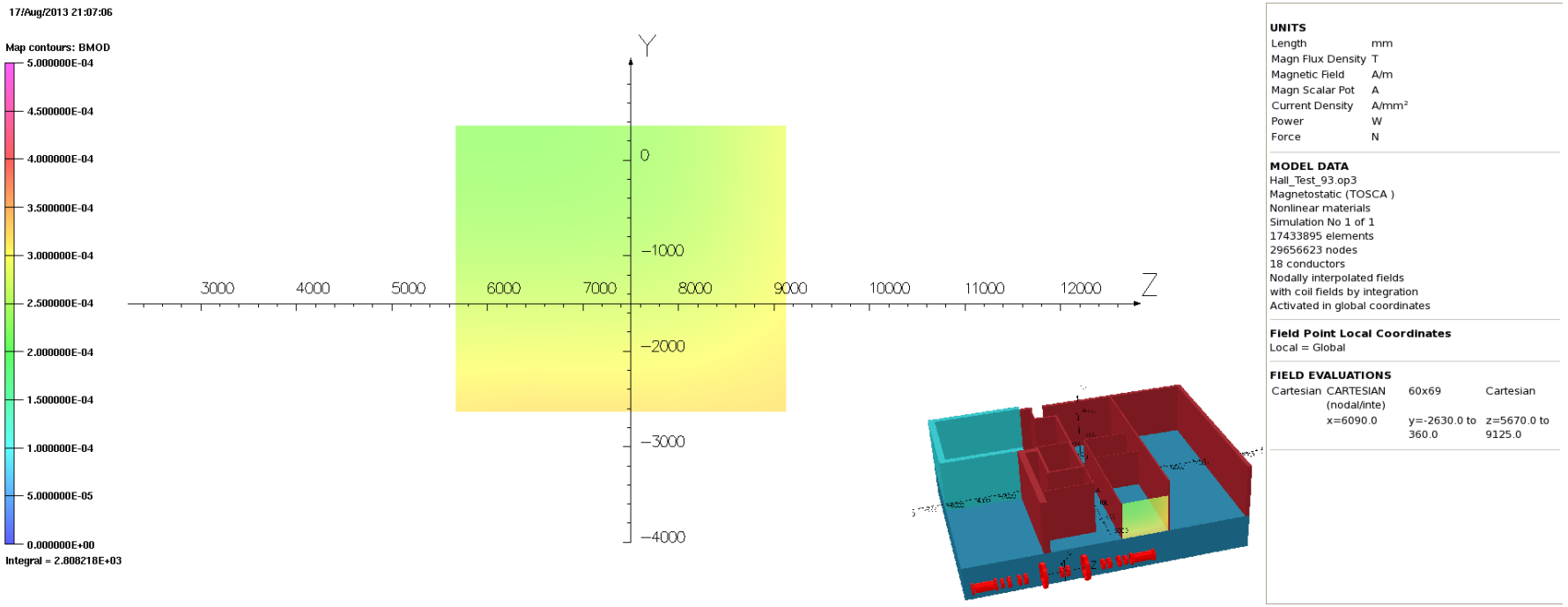

Figure 61: Bmod. Step VI 240 MeV/c Solenoid Mode. MLCR North Side.

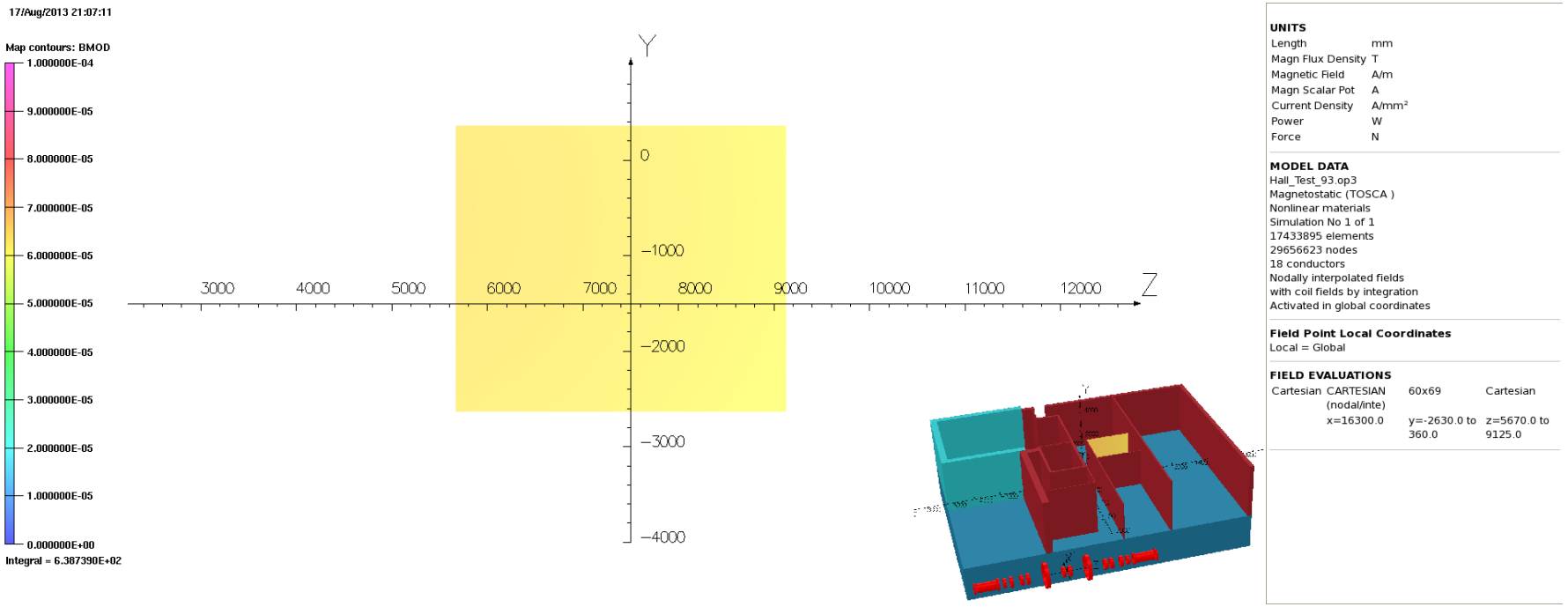

Figure 62: Bmod. Step VI 240 MeV/c Solenoid Mode. MLCR South Side. Note the different scale on this plot!

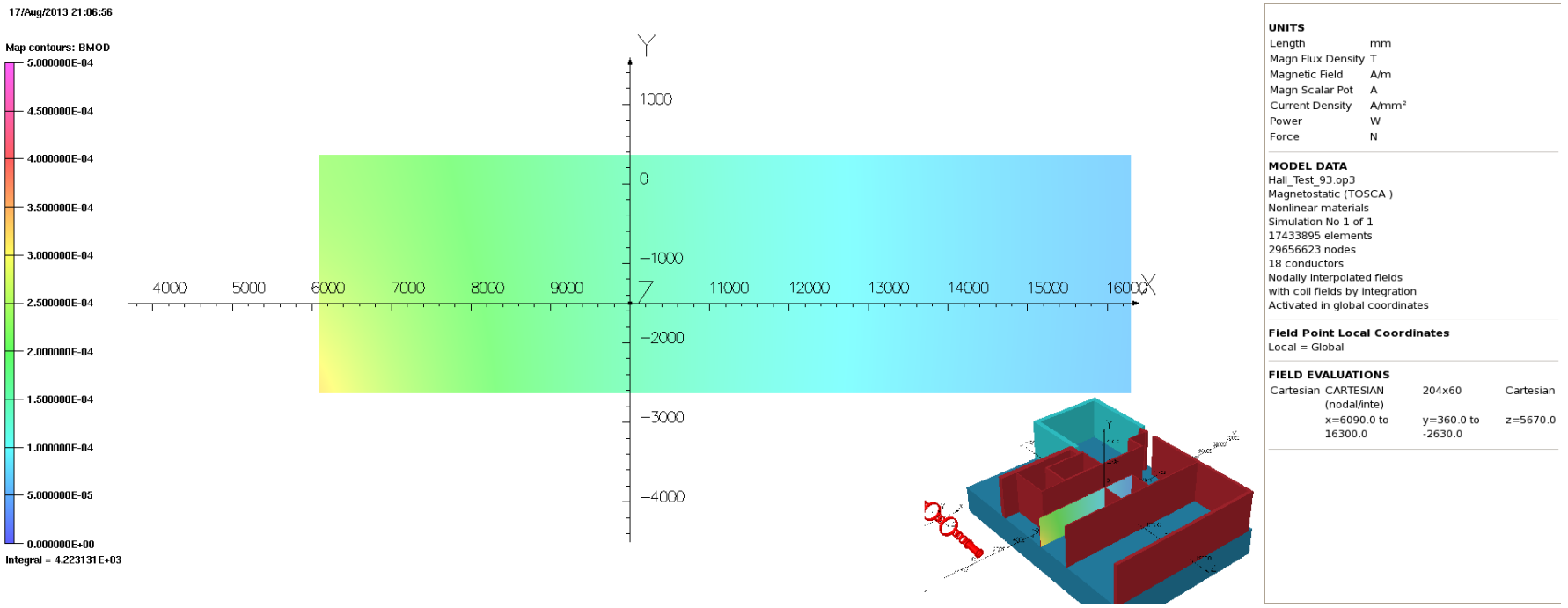

Figure 63: Bmod. Step VI 240 MeV/c Solenoid Mode. MLCR East Side.

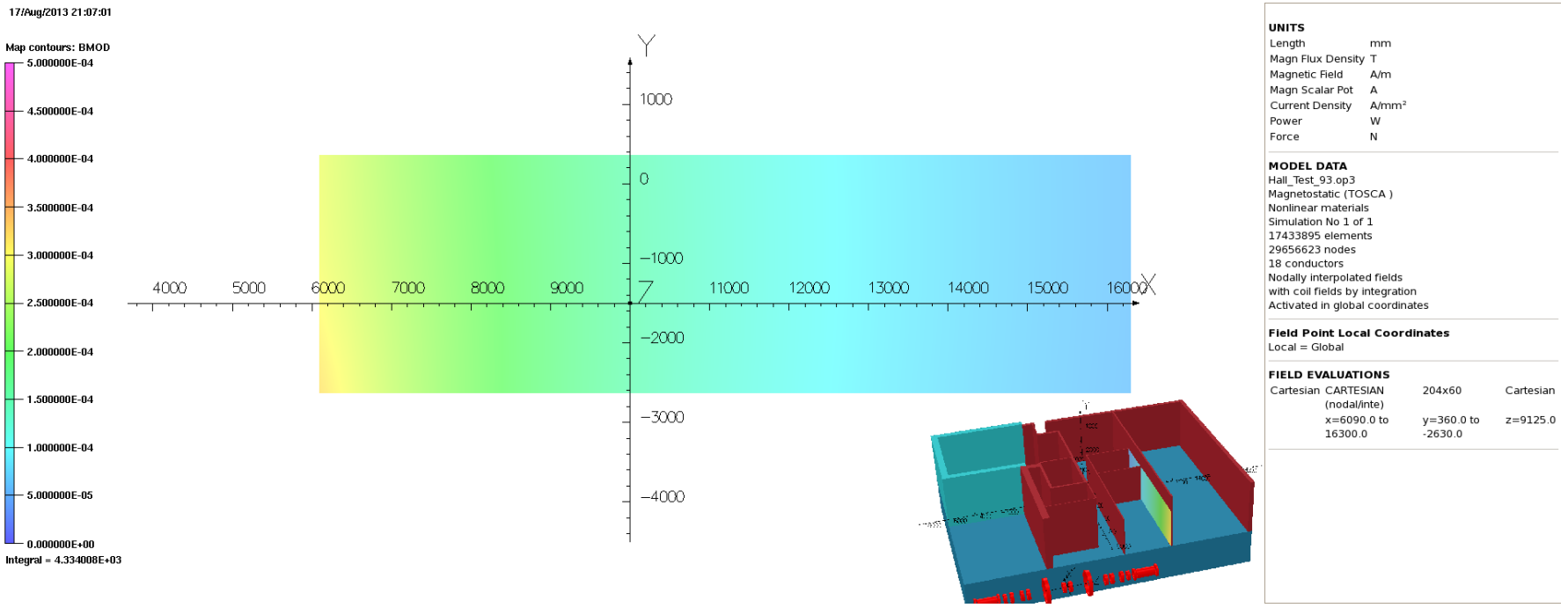

Figure 64: Bmod. Step VI 240 MeV/c Solenoid Mode. MLCR West Side.

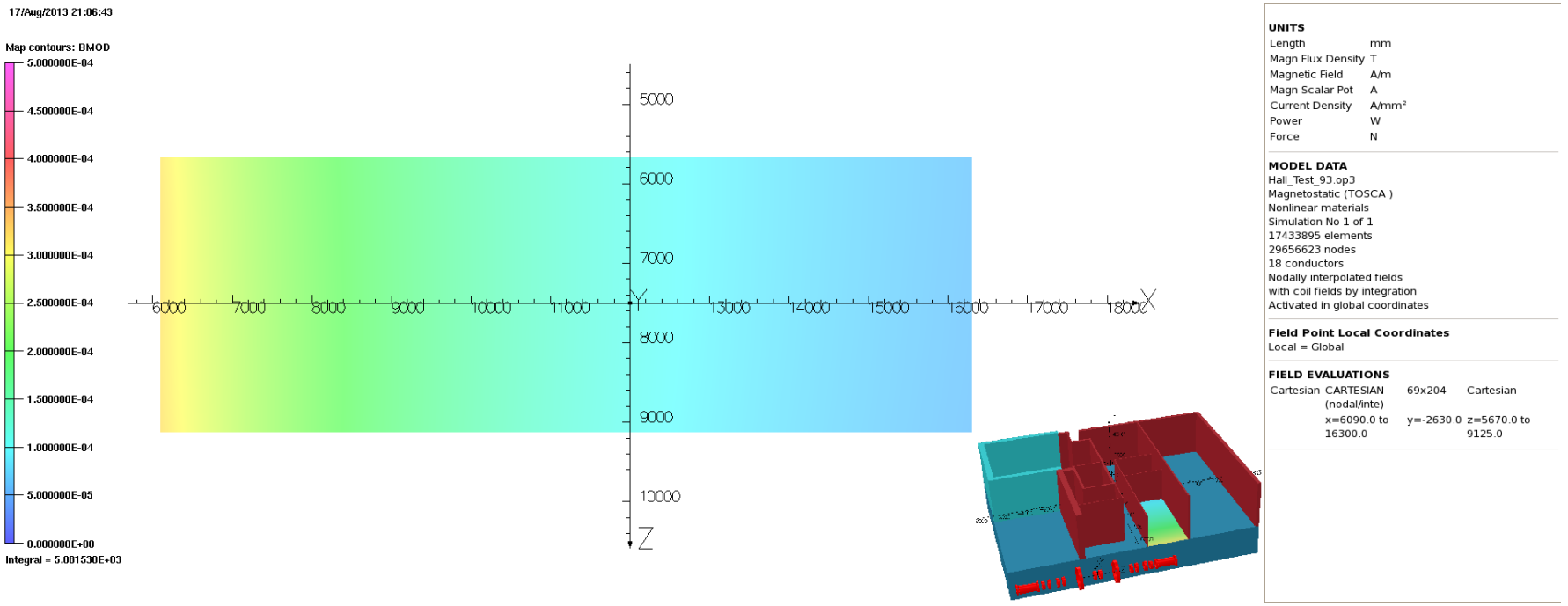

Figure 65: Bmod. Step VI 240 MeV/c Solenoid Mode. MLCR Floor.

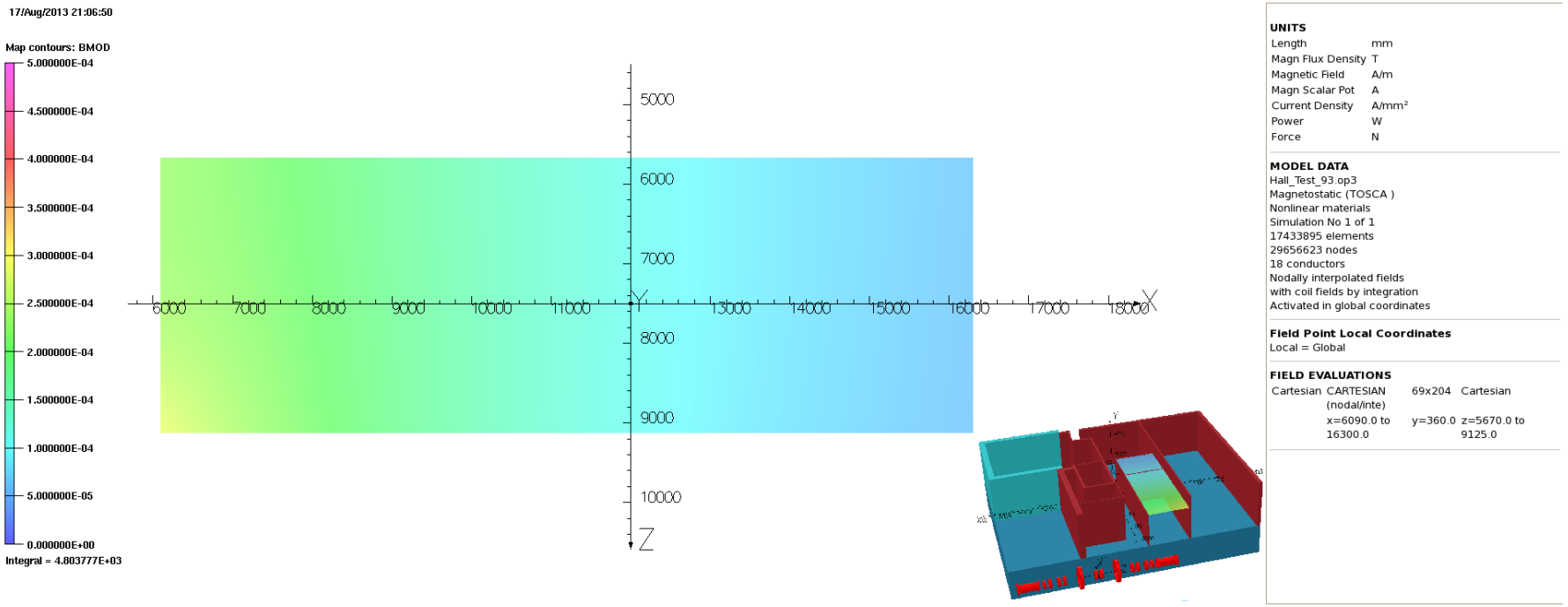

Figure 66: Bmod. Step VI 240 MeV/c Solenoid Mode. MLCR Ceiling.

E Rack Room 2 - Step VI

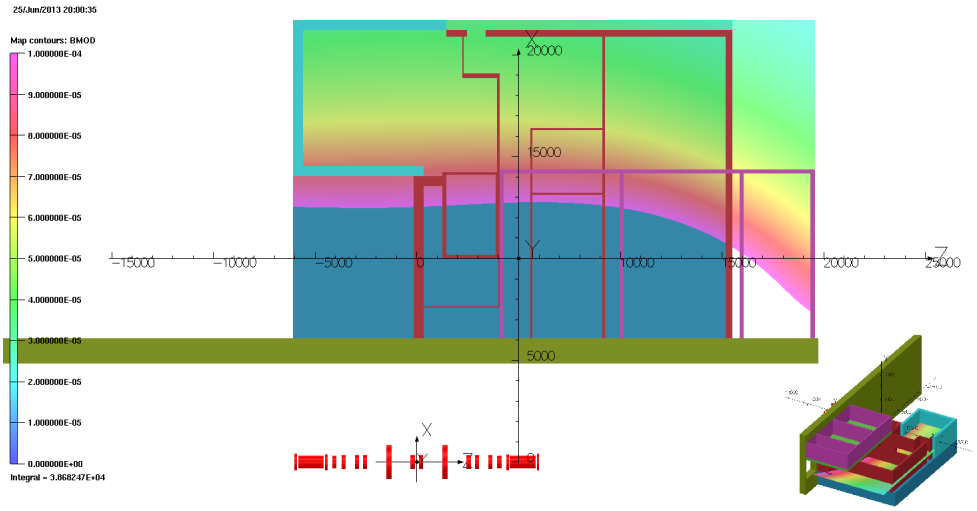

Figure 67: Bmod at y=-1000 mm. The fields through RR2 are also negligble for Step VI. Note the scale on this plot is 1 gauss.

References

[1] MICE Collaboration. MICE, an international Muon Ionisation Cooling Experiment: proposal to the Rutherford Appleton Laboratory, submitted to CCLRC and PPARC on the 10th January 2003, 2003. MICE Website - RAL Proposal.
http://www.mice.iit.edu/.

[2] MICE Collaboration. MICE technical reference document, 2004.
http://www.isis.rl.ac.uk/accelerator/MICE/TR/MICE_Tech_ref.html.